




Persistence and spread of stage-structured populations in heterogeneous landscapes

Yousef Alqawasmeh¹ · Frithjof Lutscher^{1,2} 

Received: 27 November 2017 / Revised: 10 September 2018 / Published online: 2 January 2019
© Springer-Verlag GmbH Germany, part of Springer Nature 2019

Abstract

Conditions for population persistence in heterogeneous landscapes and formulas for population spread rates are important tools for conservation ecology and invasion biology. To date, these tools have been developed for unstructured populations, yet many, if not all, species show two or more distinct phases in their life cycle. We formulate and analyze a stage-structured model for a population in a heterogeneous habitat. We divide the population into pre-reproductive and reproductive stages. We consider an environment consisting of two types of patches, one where population growth is positive, one where it is negative. Individuals move randomly within patches but can show preference towards one patch type at the interface between patches. We use linear stability analysis to determine persistence conditions, and we derive a dispersion relation to find spatial spread rates. We illustrate our results by comparing the structured population model with an appropriately scaled unstructured model. We find that a long pre-reproductive state typically increases habitat requirements for persistence and decreases spatial spread rates, but we also identify scenarios in which a population with intermediate maturation rate spreads fastest.

Keywords Structured population model · Reaction–diffusion equation · Spatial heterogeneity · Persistence condition · Critical patch size · Traveling periodic waves · Spread speed

Mathematics Subject Classification 35K37 · 35Q92 · 92D40

Frithjof Lutscher is supported by a Discovery Grant (RGPIN-2016-04795) and a Discovery Accelerator Supplement (RGPAS-2016-492872) of the Natural Sciences and Engineering Research Council of Canada.

✉ Frithjof Lutscher
flutsche@uottawa.ca
Yousef Alqawasmeh
yalqa049@uottawa.ca

¹ Department of Mathematics and Statistics, University of Ottawa, Ottawa, Canada

² Department of Biology, University of Ottawa, Ottawa, Canada

1 Introduction

Problems of population persistence and spatial spread rates are fundamental to spatial ecology. Their study through the framework of reaction–diffusion equations has not only generated a number of important ecological insights but also some deep mathematical results. The work on spatial spread phenomena started with Fisher (1937) and Kolmogorov et al. (1937), who calculated the minimal traveling wave speed, proved the existence of traveling waves and convergence to a traveling wave. Aronson and Weinberger (1975) introduced the notion of an ‘asymptotic spreading speed’ and thereby inspired a large body of literature on the topic. The ‘minimal patch-size problem’ was formulated and studied by Skellam (1951) and Kierstead and Slobodkin (1953) and has since been extended to more complicated models and applied to reserve design (Cantrell and Cosner 2003). The two cases, an unbounded homogeneous landscape and a single bounded patch, are extremes. Shigesada et al. (1986) studied a combination of the two scenarios, where a landscape consists of infinitely many patches of different quality, that alternate periodically. In this case, both questions arise: how much ‘good’ landscape is required for persistence and how fast would a population spread in a ‘traveling periodic wave’? Related analytical results for persistence and propagation in smoothly varying heterogeneous landscapes can be found in Berestycki and Hamel (2002), Berestycki et al. (2005a, b), Xin (2000). The model by Shigesada et al. with discontinuous variation in landscape quality was refined by Maciel and Lutscher (2013) to include individual movement behavior and patch preference at habitat edges.

All of these studies and many follow-up works modeled a spatially structured but physiologically unstructured population. Most actual species, however, have highly structured life cycles with reproductive rates and dispersal ability differing significantly between different stages. For example, Blanding’s turtle, a Canadian species at risk (Paterson et al. 2012), has a very long pre-reproductive stage of 14–20 years (Congdon and van Loben Sels 1991; Congdon and Van Loben Sels 1993), which has implications for the management of the species (Congdon et al. 1993). Similarly, dispersal ability and behavior can change significantly between different life stages. For example, many marine invertebrates have sessile adult stages where individuals are immobile, and also many reef fish have sedentary adults (White 2015). In some species, different life stages have different habitat preferences. For example, juveniles of western rock lobster (*Panulirus Cygnus*) choose limestone reef habitat (< 10 m from the shore), while adults prefer offshore water habitat (30–150 m) (Gillanders et al. 2003). Since reproduction and dispersal behavior are the two main ingredients that determine population persistence and spatial spread rates, we need to understand how the heterogeneity in these attributes affects model outcomes.

Non-spatial structured population models have a long history in theory and application, as matrix models with discrete stages in discrete time (Caswell 2001) and as integral equations with continuous stage distribution in continuous time (Metz and Diekmann 1986). Somewhat in between are models of discrete stages in continuous time. These models gain mathematical tractability in exchange for the simplifying assumption that stage duration is exponentially distributed. Spatially structured versions of matrix models were formulated and studied quite intensively as integrodif-

ference equations on homogeneous landscapes (Lui 1989; Neubert and Caswell 2000; Lutscher and Lewis 2004). Similarly, spatial models for physiologically structured populations were studied in a reaction–diffusion setting (Gurtin and MacCamy 1981; Hernandez 1988, 1998). A few recent works establish some more abstract mathematical properties of these kinds of models in heterogeneous landscapes (Liang and Zhao 2010), but more concrete and detailed studies on how the dynamics of structured populations in heterogeneous landscapes differs from that of unstructured populations have not been conducted.

In this paper, we formulate and analyze a minimal meaningful structured population model in a heterogeneous landscape. More specifically, we consider a structured population of two stages: a pre-reproductive juvenile stage and a reproductive adult stage. Similarly, we divide the landscape into two types of patches: a ‘good’ patch, where the local population growth rate is positive and a ‘bad’ patch, where it is negative. We model spatial movement by diffusion and include patch preference at interfaces between habitat types as presented by Maciel and Lutscher (2013). Then we analyze our model with respect to different metrics, namely the minimal patch-size (Skellam 1951) and the minimal traveling periodic wave speed (Shigesada et al. 1986). We find a number of explicit and implicit formulas for these quantities as well as expressions for their sensitivities to model parameters. We separately consider the ecologically important case of sessile adult individuals. We illustrate our results by comparing the structured model with an appropriately constructed single-stage model and highlight the importance of including stage-structure into the model equations.

2 Model derivation

Populations can be structured along many dimensions, such as age, stage, or sex. We develop our theory here using a two-stage model where individuals are classified as either non-reproductive juveniles or as reproductive adults. This distinction is the simplest meaningful extension of the common unstructured modelling approach. The generalization to more stages is straight forward but the calculations become increasingly more tedious as the number of compartments increases.

Throughout this work, we denote by $u(t)$ and $v(t)$ the density of juveniles and adults, respectively, at time t . In general, the linear model for reproduction, maturation and death reads

$$\dot{u} = rv - (m + \mu_u)u, \quad \dot{v} = mu - \mu_v v, \quad (1)$$

where r is the reproduction rate, m is the maturation rate, and $\mu_{u,v}$ are the respective death rates. All parameters are assumed positive. In this formulation, we implicitly assumed that maturation times are exponentially distributed. Other sojourn-time distributions typically require integral formulations (Thieme 2003). Stability analysis of the trivial state of model (1) gives the minimal reproductive rate required for persistence of this population as follows.

Proposition 1 *If $r > \mu_v (1 + \frac{\mu_u}{m})$ then the zero state of model (1) is unstable.*

To include space into our model, we denote the spatial location in a one-dimensional domain by x and write $u(t, x)$, $v(t, x)$ as the respective densities of juveniles and

adults. We model spatial movement by diffusion and chose the so-called ecological diffusion formulation (Turchin 1998) for random movement in heterogeneous habitats. Our model then consists of the following system of two reaction–diffusion equations with stage-dependent diffusion coefficients $D_{u,v}$.

$$\frac{\partial}{\partial t} u(t, x) = \frac{\partial^2}{\partial x^2} [D_u(x)u(t, x)] + r(x)v(t, x) - [m(x) + \mu_u(x)]u(t, x), \quad (2)$$

and

$$\frac{\partial}{\partial t} v(t, x) = \frac{\partial^2}{\partial x^2} [D_v(x)v(t, x)] + m(x)u(t, x) - \mu_v(x)v(t, x). \quad (3)$$

All parameters are allowed to be positive functions of the spatial variable but are assumed independent of time.

As formulated, the model requires an enormous amount of empirical data to obtain parameter estimates at all locations and it is too general to obtain ecologically relevant insights. Instead, we follow previous authors and impose a landscape-ecology point of view (Shigesada et al. 1986; Cruywagen et al. 1996; Maciel and Lutscher 2013; Musgrave 2013; Maciel and Lutscher 2015). In this view, a landscape consists of ‘patches’, i.e. regions in space that are relatively homogeneous within but significantly different from the neighboring region. Mathematically, this view is reflected in the assumption that all coefficient functions are piecewise constant functions in space. Moreover, we assume that there are only two types of patches. As above for the number of stages, the model formulation can be extended to more than two patch types, but explicit calculations become quite tedious.

With only two types of patches, we denote the values of the density and parameter functions by indices, i.e. we write $u_i(t, x)$ for the density of juveniles on patch type i (with $i = 1, 2$) and r_i for the value of $r(x)$ of a patch of type i , and similarly for all other densities and parameters. Hence, our model equations for x in a patch of type i read

$$\frac{\partial}{\partial t} u_i(t, x) = D_{u_i} \frac{\partial^2}{\partial x^2} u_i(t, x) + f_{u_i}(u_i, v_i), \quad (4)$$

$$\frac{\partial}{\partial t} v_i(t, x) = D_{v_i} \frac{\partial^2}{\partial x^2} v_i(t, x) + f_{v_i}(u_i, v_i), \quad (5)$$

with reaction terms

$$f_{u_i}(u_i, v_i) = r_i v_i(t, x) - [m_i + \mu_{u_i}]u_i(t, x), \quad (6)$$

$$f_{v_i}(u_i, v_i) = m_i u_i(t, x) - \mu_{v_i} v_i(t, x). \quad (7)$$

In the ecological literature a patch is called a ‘source’ if the population can grow there locally and a ‘sink’ if not. Mathematically, this distinction is characterized by Proposition 1. Accordingly, we call patch type i a ‘source’ or a ‘good patch’ if

$$r_i > \mu_{v_i} \left(1 + \frac{\mu_{u_i}}{m_i} \right), \quad (8)$$

and a ‘sink’ or ‘bad patch’ if the reverse inequality holds.

Finally, we need to characterize the behavior of individuals at the interface between two patch types. We assume that no individuals are created or destroyed as they cross from one patch into another. This assumption translates into the population fluxes being continuous across an interface. On the other hand, we allow individuals to have a preference for one or the other patch type. The derivations by Ovaskainen and Cornell (2003), Maciel and Lutscher (2013) then show that the population density across an interface need not be continuous. To illustrate, if we assume that $x = 0$ is an interface between a good patch (type 1) to the right (i.e. $x > 0$) and a bad patch (type 2) to the left (i.e. $x < 0$), and if we denote by $\alpha_u \in [0, 1]$ the probability that a juvenile individual at this interface will choose to move into the good patch, then the density and flux matching conditions for juveniles at $x = 0$ are given by

$$u_1(t, 0^+) = \lim_{x \rightarrow 0^+} u_1(t, x) = \frac{\alpha_u}{1 - \alpha_u} \frac{D_{u_2}}{D_{u_1}} \lim_{x \rightarrow 0^-} u_2(t, x) = k_u u_2(t, 0^-), \quad (9)$$

and

$$\lim_{x \rightarrow 0^+} \frac{\partial u_1}{\partial x}(t, x) = \frac{D_{u_2}}{D_{u_1}} \lim_{x \rightarrow 0^-} \frac{\partial u_2}{\partial x}(t, x), \quad (10)$$

with the dimensionless parameter combination in (9) as $k_u = \frac{\alpha_u}{1 - \alpha_u} \frac{D_{u_2}}{D_{u_1}}$. A value of $\alpha_u = 0.5$ indicates no preference and higher values of α_u indicate a preference for the good patch type. If the good patch is located on the left and the bad patch on the right, then the limits and parameters are exchanged accordingly. Corresponding interface conditions hold for the adult equation with parameter k_v defined analogously.

In the following section, we study the simplest possible non-homogeneous landscape, namely a single good patch situated in an otherwise hostile environment. By studying the stability of the trivial state, we determine the minimal patch size. In Sect. 4, we consider an infinite landscape in which good and bad patches alternate periodically, and we study the persistence conditions again by linear stability analysis. The dispersion relation for the minimal speed of a traveling periodic wave in such a landscape is studied in Sect. 5. After that, we turn to homogenization techniques to obtain simpler but approximate expressions for the spatial spread rate of the population. In the final sections, we first consider the scenario that adults are immobile (Sect. 8) and then illustrate our results by exploring specifically the importance of the maturation rate on persistence conditions and spread rates (Sect. 9).

3 Single-patch landscape

We begin the analysis of our model with the classical minimal patch-size problem, originally posed by Skellam (1951) and Kierstead and Slobodkin (1953): How large does a bounded domain surrounded by a hostile landscape have to be to ensure the persistence of a diffusing population? This set-up is a special case of the two-type environment that we described above. It results, for example, when we choose a bounded source patch bordered left and right by unbounded sink patches with arbitrarily large

mortality and/or a probability $\alpha = 0$ to stay in the source patch when reaching the boundary.

We choose a source patch of length L and drop the index i from the notation since only one patch type is involved. Hence, we study Eqs. (4) and (5) with spatially constant parameters on $x \in [0, L]$,

$$\frac{\partial}{\partial t} u = D_u \frac{\partial^2 u}{\partial x^2} + rv - (m + \mu_u)u, \tag{11}$$

$$\frac{\partial}{\partial t} v = D_v \frac{\partial^2 v}{\partial x^2} + m u - \mu_v v, \tag{12}$$

and hostile boundary conditions

$$u(t, 0) = u(t, L) = v(t, 0) = v(t, L) = 0. \tag{13}$$

Since the equations are linear, we look for exponential solutions of the form

$$\begin{bmatrix} u(t, x) \\ v(t, x) \end{bmatrix} = e^{\lambda t} \begin{bmatrix} U(x) \\ V(x) \end{bmatrix}.$$

Solutions grow if $\Re\lambda > 0$ and decline if $\Re\lambda < 0$. The population is said to persist when there is at least one eigenvalue with positive real part. By standard results for positive operators, we know that the eigenvalue with the largest real part (the ‘principal’ eigenvalue) is real and has a positive eigenfunction. The persistence boundary is given by the set of parameters for which the principal eigenvalue is $\lambda = 0$. We investigate how the persistence boundary depends on parameters.

The eigenvalue problem can be written as the following second-order system of ordinary differential equations with $x \in [0, L]$:

$$\lambda U = D_u U'' - (m + \mu_u)U + rV, \tag{14}$$

$$\lambda V = D_v V'' + mU - \mu_v V. \tag{15}$$

We use (14) to write V in terms of U and substitute the result into (15) to get the single fourth-order equation

$$D_u D_v \frac{d^4}{dx^4} U - [D_v B + (\mu_v + \lambda)D_u] \frac{d^2}{dx^2} U - [rm - (\mu_v + \lambda)B] U = 0, \tag{16}$$

with $B = m + \mu_u + \lambda$ and boundary conditions

$$U(0) = U(L) = U''(0) = U''(L) = 0.$$

The linear differential equation in (16) has the bi-quadratic characteristic equation

$$z^4 - az^2 - b = 0, \tag{17}$$

with coefficients

$$a = \frac{D_v B + (\mu_v + \lambda) D_u}{D_v D_u}, \quad b = \frac{r m - (\mu_v + \lambda) B}{D_v D_u}.$$

Equation (17) has the four roots

$$z = \pm \sqrt{\frac{a \pm (a^2 + 4b)^{\frac{1}{2}}}{2}}. \tag{18}$$

When $\lambda = 0$, we have $a > 0$. Furthermore, the condition $b > 0$ is equivalent to the inequality in (8). In other words, the patch is a good patch if and only if $b > 0$. Since a population cannot persist on an isolated sink patch, we shall only treat the case $b > 0$.

If $b > 0$ then $a + (a^2 + 4b)^{\frac{1}{2}} > 0$ and $a - (a^2 + 4b)^{\frac{1}{2}} < 0$. Hence, (17) has two real and two purely imaginary roots. We can then write the eigenfunction as

$$U(x) = C \cosh(z_1 x) + G \sinh(z_1 x) + H \cos(z_2 x) + F \sin(z_2 x), \tag{19}$$

where

$$z_1 = \sqrt{\frac{a + (a^2 + 4b)^{\frac{1}{2}}}{2}} \quad \text{and} \quad z_2 = \sqrt{\frac{(a^2 + 4b)^{\frac{1}{2}} - a}{2}}. \tag{20}$$

From the boundary conditions $U(0) = U''(0) = 0$ we obtain $C + H = 0$ and $C z_1^2 - H z_2^2 = 0$, which implies $C = H = 0$. Similarly, applying the boundary conditions $U(L) = U''(L) = 0$ implies $G = 0$ and gives the persistence boundary implicitly as $\sin(z_2 L) = 0$. We summarize these calculations as follows.

Proposition 2 *The dominant eigenvalue for model (11), (12) is zero if*

$$\sin(z_2 L) = 0. \tag{21}$$

Accordingly, the minimal patch-size is given by

$$L^* = \frac{\pi}{z_2}. \tag{22}$$

with z_2 as in (20).

From the classical results by Skellam (1951), we expect the minimal patch-size to decrease with population growth rate, which is indeed the case; see Fig. 1a. This plot also indicates that the minimal patch-size decreases with maturation rate. In Fig. 1b, we plot L^* as a function of m for different diffusion coefficients. We expect that L^* increases with diffusion, since diffusion increases boundary loss. It turns out that for the chosen parameter values, the minimal patch-size increases more when we increase adult diffusion than when we increase juvenile diffusion by the same amount.

Since we have an explicit formula for the minimal patch-size L^* in (22), we can study the dependence on parameter changes explicitly by calculating the sensitivity and elasticity of L^* with respect to each parameter. Whereas the sensitivity of L^*

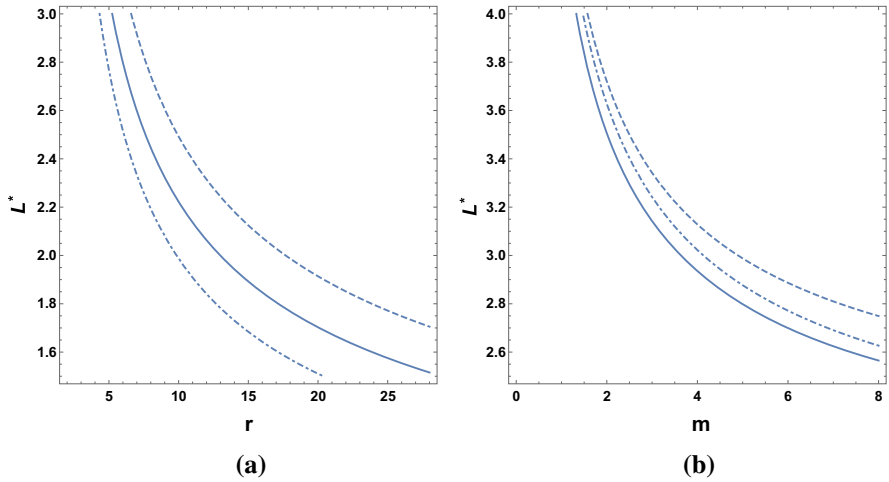


Fig. 1 Minimal patch-size for the juvenile-adult model according to expression (22). **a** L^* as a function of reproduction rate r with maturation rate $m = 3$ (dashed), $m = 5$ (solid), and $m = 9$ (dash-dot). **b** L^* as a function of m with diffusion coefficients $D_u = 2.4$ (dash-dot), or $D_v = 2.4$ (dashed). The solid curve has default parameters $D_u = D_v = 2$, also used in (a), as well as $r = 6$ and $\mu_u = \mu_v = 1$

with respect to parameter r , say, is simply the derivative of L^* with respect to r , the elasticity (or relative sensitivity) is the sensitivity multiplied by r/L^* .

The sensitivities are given explicitly as

$$\frac{\partial L^*}{\partial r} = -\frac{m\pi}{2D_u D_v (z_2)^3 \sqrt{a^2 + 4b}}, \tag{23}$$

$$\frac{\partial L^*}{\partial m} = -\frac{\pi}{4D_u D_v (z_2)^3} \left(-D_v + \frac{2(r - \mu_v) + aD_v}{\sqrt{a^2 + 4b}} \right), \tag{24}$$

$$\frac{\partial L^*}{\partial D_u} = -\frac{\pi}{4D_u D_v (z_2)^3} \left(-\mu_v + aD_v + \frac{a\mu_v - (a^2 + 2b)D_v}{\sqrt{a^2 + 4b}} \right), \tag{25}$$

$$\frac{\partial L^*}{\partial D_v} = -\frac{\pi}{4D_u D_v (z_2)^3} \left(-(m + \mu_u) + aD_u + \frac{a(\mu_u + m) - (a^2 + 2b)D_u}{\sqrt{a^2 + 4b}} \right), \tag{26}$$

$$\frac{\partial L^*}{\partial \mu_u} = -\frac{\pi}{4D_u D_v (z_2)^3} \left(-D_v + \frac{-2\mu_v + aD_v}{\sqrt{a^2 + 4b}} \right), \tag{27}$$

and

$$\frac{\partial L^*}{\partial \mu_v} = -\frac{\pi}{4D_u D_v (z_2)^3} \left(-D_u + \frac{-2(m + \mu_u) + aD_u}{\sqrt{a^2 + 4b}} \right). \tag{28}$$

We present the sensitivities and elasticities for our chosen default parameter values in Table 1. As expected from Fig. 1, L^* decreases with r and m and increases with all other parameters. The sensitivity of L^* with respect to D_v is higher than with respect to D_u . While the actual numbers in the table change with parameter values, we expect the sign pattern to persist independently of parameter values.

Table 1 Sensitivity and elasticity of the minimal patch size (L^*) with respect to default parameters: $D_u = D_v = 2$, $\mu_u = \mu_v = 1$, $r = 6$ and $m = 5$

Population parameter	Sensitivity value	Elasticity value
reproduction rate (r)	- 0.23047	- 0.494162
maturation rate (m)	- 0.114276	- 0.204187
juveniles diffusion term (D_u)	0.204547	0.146193
adults diffusion term (D_v)	0.495031	0.353807
juveniles mortality term (μ_u)	0.162287	0.057995
adults mortality term (μ_v)	0.392757	0.140355

In this section, we considered the extreme case of hostile surroundings for a source patch. We also considered other scenarios where the surrounding sink habitat is not completely hostile and/or the probability of staying in the source habitat is not zero. The details for these scenarios are given explicitly by Alqawasmeh (2017). Here, we continue with the more general case of periodic landscapes.

4 Periodic patchy landscape

The minimal patch-size from the previous section is an extreme case. Often, there is not only a single patch where the population can grow and the next good patch is not infinitely far away. In this section, we study the persistence condition of the structured population in a periodic landscape, consisting of two alternating types of habitat, one ‘good’ and one ‘bad’ according to the condition in (8). This approach was pioneered for unstructured populations by Shigesada et al. (1986), Maciel and Lutscher (2013).

We denote by L_1 and L_2 the length of the good and bad patches, respectively, and by $L = L_1 + L_2$ the period of the landscape. Without loss of generality, we pick a good patch (type 1) to be located at $(-L_1/2, L_1/2)$ and all other good patches L -periodic from thereon. Accordingly, bad patches (type 2) are located at $(L_1/2, L - L_1/2)$ and L -periodic from thereon. The model then consists of Eqs. (4, 5) on each patch together with interface conditions (9, 10) at patch interfaces $-L_1/2$ and $L_1/2$ and L -periodic from thereon.

To find the persistence conditions, we follow the same steps as in the previous section: we consider the eigenvalue problem as in (14) and (15) on each patch type separately, and transform it by differentiation into a fourth-order equation on each patch. Since we are interested in the persistence boundary only, we will set $\lambda = 0$ from here on. We arrive at the following periodic system of ordinary differential equations

$$0 = D_{u_1} D_{v_1} \frac{d}{dx^4} U_1 - [D_{v_1}(m_1 + \mu_{u_1}) + D_{u_1} \mu_{v_1}] \frac{d}{dx^2} U_1 - [r_1 m_1 - (m_1 + \mu_{u_1}) \mu_{v_1}] U_1 \tag{29}$$

for $x \in \left(\frac{-L_1}{2}, \frac{L_1}{2} \right) + L\mathbb{Z}$, and

$$0 = D_{u_2} D_{v_2} \frac{d}{dx^4} U_2 - [D_{v_2}(m_2 + \mu_{u_2}) + D_{u_2} \mu_{v_2}] \frac{d}{dx^2} U_2 - [r_2 m_2 - (m_2 + \mu_{u_2}) \mu_{v_2}] U_2 \tag{30}$$

for $x \in \left(\frac{L_1}{2}, L - \frac{L_1}{2}\right) + L\mathbb{Z}$.

Since the landscape is periodic, we are looking for periodic solutions of the same period. We can therefore restrict the analysis to one good and one bad patch and impose periodic boundary conditions.

On a good patch, Eq. (29) is the same as equation (16), and therefore, since we set $\lambda = 0$ for the persistence boundary, we obtain a general solution of the form

$$U_1(x) = B_1 \cosh(z_1 x) + C_1 \sinh(z_1 x) + G_1 \cos(z_2 x) + H_1 \sin(z_2 x), \tag{31}$$

where

$$z_1 = \sqrt{\frac{a + (a^2 + 4b)^{\frac{1}{2}}}{2}}, \quad z_2 = \sqrt{\frac{-a + (a^2 + 4b)^{\frac{1}{2}}}{2}}, \tag{32}$$

with

$$a = \frac{D_{v_1}(m_1 + \mu_{u_1}) + \mu_{v_1} D_{u_1}}{D_{u_1} D_{v_1}}, \quad b = \frac{r_1 m_1 - (m_1 + \mu_{u_1}) \mu_{v_1}}{D_{u_1} D_{v_1}}. \tag{33}$$

Since patch-type 1 is a good patch, we have $b > 0$ (see previous section), and $z_{1,2}$ are both real.

Equation (30) has the same form as (29), so that we can easily find the general solution. In addition, we can use the invariance of the equations under the reflection at $x = L/2$, i.e. under $x \mapsto L - x$ to write the solution on a bad patch as

$$U_2(x) = B_2 \cosh\left(z_3 \left(\frac{L}{2} - x\right)\right) + C_2 \sinh\left(z_3 \left(\frac{L}{2} - x\right)\right) + G_2 \cosh\left(z_4 \left(\frac{L}{2} - x\right)\right) + H_2 \sinh\left(z_4 \left(\frac{L}{2} - x\right)\right), \tag{34}$$

where

$$z_3 = \sqrt{\frac{a' + ((a')^2 + 4b')^{\frac{1}{2}}}{2}}, \quad z_4 = \sqrt{\frac{a' - ((a')^2 + 4b')^{\frac{1}{2}}}{2}}, \tag{35}$$

are the corresponding roots of the characteristic equations with a' and b' given by the same formulas as a and b in (33), except that all indices are now ‘2’ instead of ‘1’.

Since a, a' and b are positive quantities, $a^2 + 4b$ is a positive real number. Similarly, the expression $(a')^2 + 4b'$ is positive even for negative values of b' . To prove this claim, we use (33) to write $(a')^2 + 4b'$ as

$$\frac{[D_{v_2}(m_2 + \mu_{u_2}) - \mu_{v_2} D_{u_2}]^2}{(D_{v_2} D_{u_2})^2} + \frac{4r_2 m_2}{D_{v_2} D_{u_2}},$$

which is a positive real number.

We need to find conditions on the eight constants in (31) and (34) from the interface conditions. Since solutions are symmetric in the intervals $(-\frac{L_1}{2}, \frac{L_1}{2})$ and $(\frac{L_1}{2}, L - \frac{L_1}{2})$, we can equivalently study the solutions on the intervals $(0, \frac{L_1}{2})$ and $(\frac{L_1}{2}, \frac{L}{2})$, with the boundary conditions in the original variables

$$U'_1(0) = V'_1(0) = U'_2(L/2) = V'_2(L/2) = 0. \tag{36}$$

As before, we obtain the corresponding boundary conditions for $U_{1,2}$ from those for $V_{1,2}$ via

$$-r_i V_i = D_{u_i} U''_i - (m_i + \mu_{u_i}) U_i. \tag{37}$$

These conditions imply $C_1 = H_1 = C_2 = H_2 = 0$. We are down to four constants that we determine from the interface conditions at the interior interface point between the two patch types, see (9) and (10). Here, these conditions read

$$U_1 \left(\frac{L_1^-}{2} \right) = k_u U_2 \left(\frac{L_1^+}{2} \right), \quad U'_1 \left(\frac{L_1^-}{2} \right) = D_u U'_2 \left(\frac{L_1^+}{2} \right), \tag{38}$$

and

$$V_1 \left(\frac{L_1^-}{2} \right) = k_v V_2 \left(\frac{L_1^+}{2} \right), \quad V'_1 \left(\frac{L_1^-}{2} \right) = D_v V'_2 \left(\frac{L_1^+}{2} \right), \tag{39}$$

where $D_u = \frac{D_{u_2}}{D_{u_1}}$, $D_v = \frac{D_{v_2}}{D_{v_1}}$, $k_{u,v}$ stand for the terms $k_u = \frac{\alpha_u}{1-\alpha_u} \frac{D_{u_2}}{D_{u_1}}$, as in (9) and similarly for k_v .

Applying the interface conditions (38)–(39), we get the four equations

$$B_1 \cosh \left(\frac{z_1 L_1}{2} \right) + G_1 \cos \left(\frac{z_2 L_1}{2} \right) = k_u \left[B_2 \cosh \left(\frac{z_3 L_2}{2} \right) + G_2 \cosh \left(\frac{z_4 L_2}{2} \right) \right], \tag{40}$$

$$\begin{aligned} & z_1 B_1 \sinh \left(\frac{z_1 L_1}{2} \right) - z_2 G_1 \sin \left(\frac{z_2 L_1}{2} \right) \\ &= D_u \left[-z_3 B_2 \sinh \left(\frac{z_3 L_2}{2} \right) - z_4 G_2 \sinh \left(\frac{z_4 L_2}{2} \right) \right], \end{aligned} \tag{41}$$

$$\begin{aligned} 0 &= B_1 \cosh \left(\frac{z_1 L_1}{2} \right) \left[r D_{u_1} (z_1)^2 - r A \right] - G_1 \cos \left(\frac{z_2 L_1}{2} \right) \left[r D_{u_1} (z_2)^2 + r A \right] \\ &+ B_2 \cosh \left(\frac{z_3 L_2}{2} \right) \left[k_v B - k_v D_{u_2} (z_3)^2 \right] + G_2 \cosh \left(\frac{z_4 L_2}{2} \right) \left[k_v B - k_v D_{u_2} (z_4)^2 \right], \end{aligned} \tag{42}$$

and

$$\begin{aligned} 0 &= B_1 \sinh \left(\frac{z_1 L_1}{2} \right) \left[r D_{u_1} (z_1)^3 - r A z_1 \right] + G_1 \sin \left(\frac{z_2 L_1}{2} \right) \left[r D_{u_1} (z_2)^3 + r A z_2 \right] \\ &+ B_2 D_v \sinh \left(\frac{z_3 L_2}{2} \right) \left[D_{u_2} (z_3)^3 - B z_3 \right] + G_2 D_v \sinh \left(\frac{z_4 L_2}{2} \right) \left[D_{u_2} (z_4)^3 - B z_4 \right], \end{aligned} \tag{43}$$

where $A = (m_1 + \mu_{u_1})$ and $B = (m_2 + \mu_{u_2})$.

We write these linear equations as a matrix for the remaining constants. The matrix is too large to display here, but it can be found in the work by Alqawasmeh (2017). For a non-trivial solution of (40) and (43) to exist, the determinant of this matrix must equal zero. We explicitly calculated this condition to be

$$\begin{aligned}
 0 = & z_3 z_2 \left(-BD_v + AD_u r + D_{u_2} z_2^2 r + D_v D_{u_2} z_3^2 \right) \\
 & \times \left(Bk_v - Ak_u r + D_{u_1} k_u r z_1^2 - D_{u_2} k_v z_4^2 \right) \tan \left(\frac{z_2 L_1}{2} \right) \tanh \left(\frac{z_3 L_2}{2} \right) \\
 & + z_4 z_3 \left(D_{u_2} \right)^2 D_v r \left(z_1^2 + z_2^2 \right) \left(z_4^2 - z_3^2 \right) \tanh \left(\frac{z_4 L_2}{2} \right) \tanh \left(\frac{z_3 L_2}{2} \right) \\
 & + z_1 z_2 r D_{u_1} D_{u_2} k_v k_u \left(z_2^2 + z_1^2 \right) \left(z_3^2 - z_4^2 \right) \tanh \left(\frac{z_1 L_1}{2} \right) \tan \left(\frac{z_2 L_1}{2} \right) \\
 & + z_1 z_4 \left(-r D_{u_2} z_1^2 + r A D_u - D_v B + D_v D_{u_2} z_4^2 \right) \\
 & \times \left(Ak_u r - Bk_v + D_{u_1} k_u r z_2^2 + D_{u_2} k_v z_3^2 \right) \tanh \left(\frac{z_1 L_1}{2} \right) \tanh \left(\frac{z_4 L_2}{2} \right) \\
 & + z_1 z_3 \left(r D_{u_2} z_1^2 - A D_u r + D_v B - D_v D_{u_2} z_3^2 \right) \\
 & \times \left(-Bk_v + Ak_u r + D_{u_1} k_u r z_2^2 + D_{u_2} k_v z_4^2 \right) \tanh \left(\frac{z_1 L_1}{2} \right) \tanh \left(\frac{z_3 L_2}{2} \right) \\
 & - z_2 z_4 \left(-BD_v + D_v D_{u_2} z_4^2 + r A D_u + r D_{u_2} z_2^2 \right) \\
 & \times \left(Bk_v - Ak_u r + D_{u_1} k_u r z_1^2 - D_{u_2} k_v z_3^2 \right) \tan \left(\frac{z_2 L_1}{2} \right) \tanh \left(\frac{z_4 L_2}{2} \right) \quad (44)
 \end{aligned}$$

where $D_u = \frac{D_{u_2}}{D_{u_1}}$, $D_v = \frac{D_{v_2}}{D_{v_1}}$, $r = \frac{r_2}{r_1}$, $A = (m_1 + \mu_{u_1})$ and $B = (m_2 + \mu_{u_2})$.

Proposition 3 Model (4,5) has a zero eigenvalue if the relation in (44) is satisfied.

The proposition gives us a necessary but not sufficient condition to locate the persistence boundary. Indeed, if one plots the expression in (44) as a function of, say $L_1 > 0$, while all other parameters are fixed, one will find infinitely many zeros. From biological considerations, one would expect that the smallest such positive L_1 corresponds to the actual persistence boundary. Mathematically, one has to ensure that the corresponding eigenfunction is of one sign. This requirement was obviously satisfied for the case in Proposition 2. Previous authors (Lutscher et al. 2006; Maciel and Lutscher 2013; Shigesada et al. 1986) picked the smallest positive zero with respect to L_1 without any further justification. We give the justification for our model in the next proposition.

Proposition 4 The critical patch-size, L^* , is given by the smallest positive value of L_1 such that (44) is satisfied.

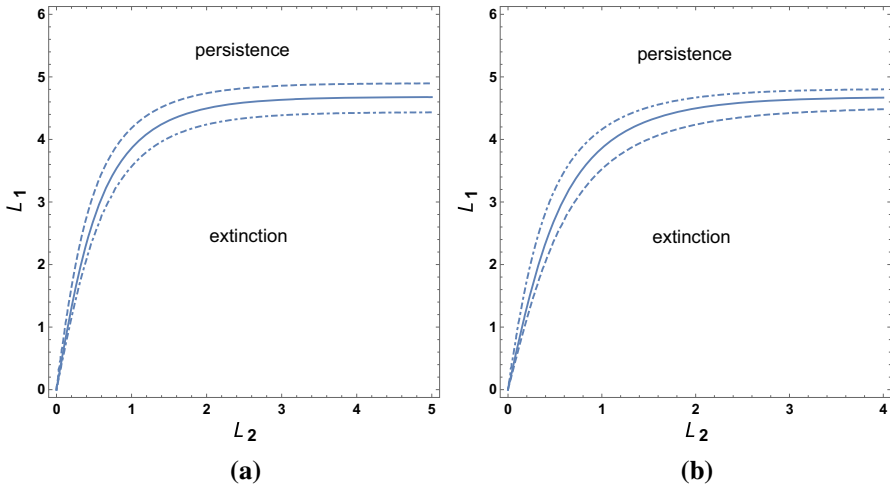


Fig. 2 Persistence boundary according to (44) for the juveniles-adults model in a periodic heterogeneous landscape as a function of good patch size L_1 and bad patch size L_2 . **a** Juveniles habitat preference varies from $\alpha_u = 0.5$ (solid curve), and $\alpha_u = 0.25$ (dashed curve) to $\alpha_u = 0.75$ (dash-dot curve). **b** Juveniles diffusion coefficient in the bad patch varies from $D_{u_2} = 1$ (solid curve), and $D_{u_2} = 4$ (dashed curve) to $D_{u_2} = 0.25$ (dash-dot curve). Default parameters are $r_1 = 2, r_2 = 0.2, \mu_{u_1} = \mu_{v_1} = 1, \mu_{u_2} = \mu_{v_2} = 2, D_{u_1} = D_{v_1} = 2, D_{v_2} = 1, m_1 = 5,$ and $m_2 = 1$. In **b** we assume that individuals have no habitat preference, and so $\alpha_u = \alpha_v = 0.5$

We give the proof of this proposition in the ‘‘Appendix’’. Here, we illustrate the dependence of L^* on various model parameters. For example, the chance of the population to persist increases with juveniles’ habitat preference (Fig. 2a), and also increases with diffusion in bad patches (Fig. 2b). Since diffusion increases individuals’ transition between patches, we expect that diffusion in good patches have a decreasing influence on population persistence.

5 Minimal speed of traveling periodic waves

When the persistence conditions from the previous section are satisfied, we expect that the population will spread in space if introduced locally. We derive and study the dispersion relation that gives us the minimal speed of a traveling periodic wave (TPW) for the linear system (Shigesada et al. 1986). In many cases, this minimal speed is also the so-called spreading speed, i.e. the speed at which a locally introduced population spreads in the non-linear equation (Weinberger et al. 2002; Zhao 2009). For brevity, we will use the term ‘spread speed’ interchangeably with minimal speed of a TPW.

We assume that the landscape consists of infinitely many, periodically alternating patches of two types, namely ‘good’ and ‘bad’ according to the population growth rate in (8). As above, L_1 and L_2 represent size of the good and bad patch, respectively, and $L = L_1 + L_2$ represents the spatial period. The equations are the same as in the previous section.

We substitute into the equations the standard ansatz of a TPW the form

$$u(t, x) = \phi(z)g(x), \quad v(t, x) = \tilde{\phi}(z)\tilde{g}(x), \quad z = x - Ct, \tag{45}$$

where the velocity C can be written as $C = L/t^*$ and t^* is the time required for traveling one spatial period (Shigesada et al. 1986). We are looking for rightward traveling waves and therefore require $\phi(z), \tilde{\phi}(z) \rightarrow 0$ as $z \rightarrow \infty$. Since we seek periodic solutions, we require $g(x) = g(x + L)$ and $\tilde{g}(x) = \tilde{g}(x + L)$.

If we substitute the ansatz in (45) into Eqs. (2, 3), we get $\phi(z) \sim e^{-sz}$ and $\tilde{\phi}(z) \sim e^{-sz}$, $s > 0$. Hence, we can write $u(t, x)$ and $v(t, x)$ as

$$u(t, x) = e^{-sz}g(x), \quad v(t, x) = e^{-sz}\tilde{g}(x). \tag{46}$$

We write $g = g_{1,2}$ and $\tilde{g} = \tilde{g}_{1,2}$ on good and bad patches, respectively.

We will now derive equations for functions g, \tilde{g} . Similarly to before, these will be linear fourth-order equations so that the solutions will have four free parameters each. We then use the interface conditions to determine the conditions on the eight parameters for a non-trivial solution to exist. This existence condition will result in a relationship between the shape parameter s and the speed C : the so-called dispersion relation $C = C(s)$. To find the minimal speed of a TPW, we then minimize this expression over positive s and obtain the ‘spread speed’ $C^* = \min_{s>0} C(s)$.

With the ansatz in (46), the equation in (2) becomes

$$sC e^{-s(x-Ct)} g_1(x) = D_{u_1}[\phi_1''(z)g_1(x) + \phi_1(z)g_1''(x) + 2\phi_1'(z)g_1'(x)] + r_1\tilde{\phi}_1(z)\tilde{g}_1(x) - (m_1 + \mu_{u_1})\phi_1(z)g_1(x). \tag{47}$$

The exponentials can be canceled so that we obtain

$$sC g_1(x) = D_{u_1}[s^2 g_1(x) + g_1''(x) - 2s g_1'(x)] + r_1 \tilde{g}_1(x) - (m_1 + \mu_{u_1}) g_1(x). \tag{48}$$

Similarly, Eq. (3) becomes

$$sC \tilde{g}_1(x) = D_{v_1} [s^2 \tilde{g}_1(x) + \tilde{g}_1''(x) - 2s \tilde{g}_1'(x)] + m_1 g_1(x) - \mu_{v_1} \tilde{g}_1(x). \tag{49}$$

From (48), we write $\tilde{g}_1(x)$ explicitly as follows

$$\tilde{g}_1(x) = \frac{-D_{u_1} g_1''(x) + 2s D_{u_1} g_1'(x) + (sC + m_1 + \mu_{u_1} - s^2 D_{u_1}) g_1(x)}{r_1}. \tag{50}$$

Then we substitute $\tilde{g}_1(x), \tilde{g}_1'(x),$ and $\tilde{g}_1''(x)$ into (49) to get

$$0 = -D_{v_1} D_{u_1} g_1^{(4)}(x) + 4s D_{v_1} D_{u_1} g_1^{(3)}(x) + (D_{u_1} \alpha + D_{v_1} \beta - 4s^2 D_{u_1} D_{v_1}) g_1''(x) + g_1'(x) (-2s D_{u_1} \alpha - 2s D_{v_1} \beta) + g_1(x) (r_1 m_1 - \alpha \beta), \tag{51}$$

where $\alpha = (sC + \mu_{v_1} - s^2 D_{v_1})$ and $\beta = (sC + m_1 + \mu_{u_1} - s^2 D_{u_1})$.

Dividing the equation in (51) by $(-D_{v_1} D_{u_1})$ gives the following ordinary differential equation

$$g_1^{(4)}(x) - 4s g_1^{(3)}(x) - \left(\frac{\alpha}{D_{v_1}} + \frac{\beta}{D_{u_1}} - 4s^2 \right) g_1''(x) + \left(\frac{2s\alpha}{D_{v_1}} + \frac{2s\beta}{D_{u_1}} \right) g_1'(x) - \frac{(r_1 m_1 - \alpha\beta)}{D_{v_1} D_{u_1}} g_1(x) = 0. \tag{52}$$

We need to find conditions for this equation to have non-trivial solutions.

The characteristic equation for (52) can be written as

$$z^4 - 4s z^3 - \left(\frac{\alpha}{D_{v_1}} + \frac{\beta}{D_{u_1}} - 4s^2 \right) z^2 + \left(\frac{2s\alpha}{D_{v_1}} + \frac{2s\beta}{D_{u_1}} \right) z - \frac{(r_1 m_1 - \alpha\beta)}{D_{v_1} D_{u_1}} = 0.$$

The roots of this equation are of the form

$$z = s \pm \frac{1}{\sqrt{2D_{u_1} D_{v_1}}} \sqrt{D_{v_1}(m_1 + sC + \mu_{u_1}) + D_{u_1}(sC + \mu_{v_1}) \pm \Delta_1}, \tag{53}$$

where

$$\Delta_1 = \sqrt{[D_{v_1}(m_1 + sC + \mu_{u_1}) - D_{u_1}(sC + \mu_{v_1})]^2 + 4D_{u_1} D_{v_1} r_1 m_1}.$$

The form of the solution of the differential equation (52) depends on the sign of the quantity

$$D_{v_1}(m_1 + sC + \mu_{u_1}) + D_{u_1}(sC + \mu_{v_1}) - \Delta_1. \tag{54}$$

This expression is negative if and only if

$$C < \frac{-(m_1 + \mu_{u_1} + \mu_{v_1}) + \sqrt{(m_1 + \mu_{u_1} + \mu_{v_1})^2 - 4(\mu_{u_1}\mu_{v_1} + m_1\mu_{v_1} - r_1 m_1)}}{2s}, \tag{55}$$

or equivalently, if

$$r_1 > \frac{(m_1 + sC + \mu_{u_1})(sC + \mu_{v_1})}{m_1}. \tag{56}$$

Before we continue, we note that the exact same procedure applied to the equation in bad patches leads to the differential equation for $g_2(x)$ as

$$g_2^{(4)}(x) - 4s g_2^{(3)}(x) - \left(\frac{\gamma}{D_{v_2}} + \frac{\delta}{D_{u_2}} - 4s^2 \right) g_2''(x) + \left(\frac{2s\gamma}{D_{v_2}} + \frac{2s\delta}{D_{u_2}} \right) g_2'(x) - \frac{(r_2 m_2 - \gamma\delta)}{D_{v_2} D_{u_2}} g_2(x) = 0, \tag{57}$$

where $\gamma = (sC + \mu_{v_2} - s^2 D_{v_2})$ and $\delta = (sC + m_2 + \mu_{u_2} - s^2 D_{u_2})$.

Similarly to above, there is a quartic characteristic equation, and the form of solutions of the differential equation depend on the signs of the roots of the quartic.

In bad patches, according to Proposition 1 and since $s, C > 0$, we have the inequality

$$r_2 < \frac{\mu_{v_2}(m_2 + \mu_{u_2})}{m_2} < \frac{(m_2 + sC + \mu_{u_2})(sC + \mu_{v_2})}{m_2}. \quad (58)$$

Hence, the reverse inequality of (56) holds unconditionally. Therefore, solutions of the differential equation (57) will be of the form

$$g_2(x) = e^{sx} [A' \cosh(z_3x) + B' \sinh(z_3x) + G' \cosh(z_4x) + H' \sinh(z_4x)], \quad (59)$$

where

$$z_3 = \frac{1}{\sqrt{2D_{u_2}D_{v_2}}} \sqrt{D_{v_2}(m_2 + sC + \mu_{u_2}) + D_{u_2}(sC + \mu_{v_2}) - \Delta_2},$$

$$z_4 = \frac{1}{\sqrt{2D_{u_2}D_{v_2}}} \sqrt{D_{v_2}(m_2 + sC + \mu_{u_2}) + D_{u_2}(sC + \mu_{v_2}) + \Delta_2},$$

and

$$\Delta_2 = \sqrt{[D_{v_2}(m_2 + sC + \mu_{u_2}) - D_{u_2}(sC + \mu_{v_2})]^2 + 4D_{u_2}D_{v_2}r_2m_2}.$$

In good patches, we have to distinguish cases, depending on whether (56) holds or not. If it holds, we can write the solution of the differential equation (52) as

$$g_1(x) = e^{sx} [A \cos(z_1x) + B \sin(z_1x) + G \cosh(z_2x) + H \sinh(z_2x)], \quad (60)$$

where

$$z_1 = \frac{1}{\sqrt{2D_{u_1}D_{v_1}}} \sqrt{-D_{v_1}(m_1 + sC + \mu_{u_1}) - D_{u_1}(sC + \mu_{v_1}) + \Delta_1},$$

$$z_2 = \frac{1}{\sqrt{2D_{u_1}D_{v_1}}} \sqrt{D_{v_1}(m_1 + sC + \mu_{u_1}) + D_{u_1}(sC + \mu_{v_1}) + \Delta_1},$$

and

$$\Delta_1 = \sqrt{[D_{v_1}(m_1 + sC + \mu_{u_1}) - D_{u_1}(sC + \mu_{v_1})]^2 + 4D_{u_1}D_{v_1}r_1m_1}.$$

If the reverse inequality holds, we can use hyperbolic-trigonometric formulas to convert between the two (Shigesada et al. 1986).

Equations (59) and (60) have 8 constants. To find their values, we use the interface conditions at $x = 0$ and $x = L_1$

$$g_1(0^+) = k_u g_2(0^-), \quad g_1(L_1^-) = k_u g_2(-L_2^+), \quad (61)$$

$$g'_1(0^+) - sg_1(0^+) = D_u [g'_2(0^-) - sg_2(0^-)], \tag{62}$$

$$g'_1(L_1^-) - sg_1(L_1^-) = D_u [g'_2(-L_2^+) - sg_2(-L_2^+)], \tag{63}$$

$$\tilde{g}_1(0^+) = k_v \tilde{g}_2(0^-), \quad \tilde{g}_1(L_1^-) = k_v \tilde{g}_2(-L_2^+), \tag{64}$$

$$\tilde{g}'_1(0^+) - s\tilde{g}'_1(0^+) = D_v [\tilde{g}'_2(0^-) - s\tilde{g}'_2(0^-)], \tag{65}$$

and

$$\tilde{g}'_1(L_1^-) - s\tilde{g}'_1(L_1^-) = D_v [\tilde{g}'_2(-L_2^+) - s\tilde{g}'_2(-L_2^+)]. \tag{66}$$

The interface conditions (61)–(66) produce the following system of linear equations

$$A + G = k_u(A' + G'), \tag{67}$$

$$z_1B + z_2H = D_u(z_3B' + z_4H'). \tag{68}$$

$$\begin{aligned} e^{sL} [A \cos(z_1L_1) + B \sin(z_1L_1) + G \cosh(z_2L_1) + H \sinh(z_2L_1)] \\ = k_u [A' \cosh(z_3L_2) - B' \sinh(z_3L_2) + G' \cosh(z_4L_2) - H' \sinh(z_4L_2)], \end{aligned} \tag{69}$$

$$\begin{aligned} e^{sL} [-z_1A \sin(z_1L_1) + z_1B \cos(z_1L_1) + z_2G \sinh(z_2L_1) + z_2H \cosh(z_2L_1)] \\ = D_u [-z_3A' \sinh(z_3L_2) + z_3B' \cosh(z_3L_2) \\ - z_4G' \sinh(z_4L_2) + z_4H' \cosh(z_4L_2)], \end{aligned} \tag{70}$$

$$\begin{aligned} 0 = A [D_{u_1}s^2 + D_{u_1}z_1^2 + \beta] r + G [D_{u_1}s^2 - D_{u_1}z_2^2 + \beta] r \\ + A' [-D_{u_2}s^2 + D_{u_2}z_3^2 - \delta] k_v + G' [-D_{u_2}s^2 + D_{u_2}z_4^2 - \delta] k_v, \end{aligned} \tag{71}$$

$$\begin{aligned} 0 = B [D_{u_1}z_1^3 + D_{u_1}s^2z_1 + \beta z_1] r + H [-D_{u_1}z_2^3 + D_{u_1}s^2z_2 + \beta z_2] r \\ + B' [D_{u_2}z_3^3 - D_{u_2}s^2z_3 - \delta z_3] D_v + H' [D_{u_2}z_4^3 - D_{u_2}s^2z_4 - \delta z_4] D_v, \end{aligned} \tag{72}$$

$$\begin{aligned} 0 = A [D_{u_1}z_1^2 + D_{u_1}s^2 + \beta] r e^{sL} \cos(z_1L_1) \\ + B [D_{u_1}z_1^2 + D_{u_1}s^2 + \beta] r e^{sL} \sin(z_1L_1) \\ + G [-D_{u_1}z_2^2 + D_{u_1}s^2 + \beta] r e^{sL} \cosh(z_2L_1) \\ + H [-D_{u_1}z_2^2 + D_{u_1}s^2 + \beta] r e^{sL} \sinh(z_2L_1) \\ + A' [D_{u_2}z_3^2 - D_{u_2}s^2 - \delta] k_v \cosh(z_3L_2) \\ + B' [-D_{u_2}z_3^2 + D_{u_2}s^2 + \delta] k_v \sinh(z_3L_2) \\ + G' [D_{u_2}z_4^2 - D_{u_2}s^2 - \delta] k_v \cosh(z_4L_2) \\ + H' [-D_{u_2}z_4^2 + D_{u_2}s^2 + \delta] k_v \sinh(z_4L_2), \end{aligned} \tag{73}$$

and

$$\begin{aligned}
0 = & A \left[-D_{u_1} s^2 - D_{u_1} z_1^2 - \beta \right] r z_1 e^{sL} \sin(z_1 L_1) \\
& + B \left[D_{u_1} s^2 + D_{u_1} z_1^2 + \beta \right] r z_1 e^{sL} \cos(z_1 L_1) \\
& + G \left[D_{u_1} s^2 - D_{u_1} z_2^2 + \beta \right] r z_2 e^{sL} \sinh(z_2 L_1) \\
& + H \left[D_{u_1} s^2 - D_{u_1} z_2^2 + \beta \right] r z_2 e^{sL} \cosh(z_2 L_1) \\
& + A' \left[D_{u_2} s^2 - D_{u_2} z_3^2 + \delta \right] D_v z_3 \sinh(z_3 L_2) \\
& + B' \left[-D_{u_2} s^2 + D_{u_2} z_3^2 - \delta \right] D_v z_3 \cosh(z_3 L_2) \\
& + G' \left[D_{u_2} s^2 - D_{u_2} z_4^2 + \delta \right] D_v z_4 \sinh(z_4 L_2) \\
& + H' \left[-D_{u_2} s^2 + D_{u_2} z_4^2 - \delta \right] D_v z_4 \cosh(z_4 L_2). \tag{74}
\end{aligned}$$

Equations (67)–(74) can be written in matrix form as a linear homogeneous system for the eight constants. The matrix is too large to be displayed here but can be found in the work by Alqawasmeh (2017). The system has a nontrivial solution exactly if the determinant of the coefficient matrix is zero. The explicit expression of the determinant is similarly unwieldy for display here but also available in the work by Alqawasmeh (2017). We used the symbolic computation package MATHEMATICA[®] to evaluate the expression and find the minimal speed for a traveling periodic wave.

Proposition 5 *The dispersion relation $C = C(s)$ for a traveling periodic wave is given implicitly by setting the determinant of the coefficient matrix of Eqs. (67)–(74) equal to zero.*

We now calculate the speed as the minimum of the dispersion relation, i.e. $C^* = \inf_{s>0} C(s)$. In doing so, we make the assumption that the corresponding eigenfunction is of one sign. This assumption is consistent with analytical results for related, simpler models, and we checked this assumption numerically in all figures, but we leave its proof as a future challenge.

There are several other related analytical challenges that we leave for future work. One is to show that $C(s)$ and hence C^* are positive whenever the population can persist according to Proposition 4. We checked this property numerically in all our cases. Another challenge is to consider a ‘suitable’ nonlinear version of our model and study the existence of a spreading speed, of traveling waves, and the linear conjecture for the nonlinear model. By ‘suitable’ we mean that there is no Allee effect and that the linearization of the nonlinear model reduces to our linear model. When there is an Allee effect, Maciel and Lutscher (2015) showed that a population may persist in a patchy landscape yet not spread.

In Fig. 3a, we plot the spread speed, $C^* = \inf_{s>0} C(s)$, as a function of bad patch size, L_2 , for different values of good patch size, L_1 . As expected, the plot indicates that the speed decreases with bad patch size. Similarly, the speed increases with reproduction rate in good patches; see Fig. 3b.

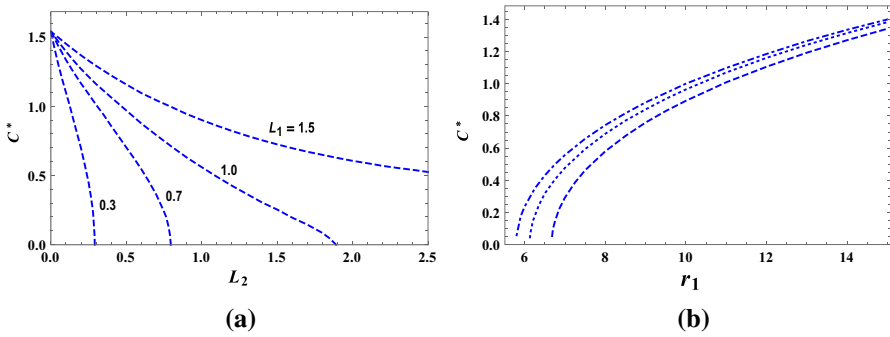


Fig. 3 Minimal traveling wave speed for the juveniles-adults model in a patchy landscape. **a** Speed decreases with bad patch size L_2 for different values of good patch size L_1 . **b** Speed increases with reproduction in the good patch for different juvenile habitat preference $\alpha_u = 0.4$ (dotted), $\alpha_u = 0.25$ (dashed) or the default value $\alpha_u = 0.5$ (dash-dot). The other parameter values are $\alpha_v = 0.5$, as well as $r_1 = 7$, $r_2 = 0.2$, $L_1 = 1$, $L_2 = 1$, $D_{u1} = D_{v1} = 0.5$, $D_{u2} = D_{v2} = 0.5$, $\mu_{u1} = \mu_{v1} = 1$, $\mu_{u2} = \mu_{v2} = 2$, and $m_1 = m_2 = 1$

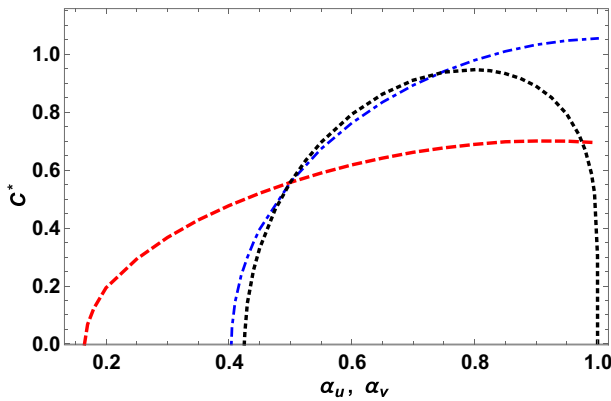


Fig. 4 Minimal traveling wave speed for juveniles-adults model in patchy landscapes as a function of habitat preference of juveniles, α_u , (dashed curve) with constant $\alpha_v = 0.5$, habitat preference of adults, α_v , (dash-dot curve) with constant $\alpha_u = 0.5$, and equal habitat preference of both, $\alpha_u = \alpha_v$, (dotted curve). Parameters are $L_1 = 1 = L_2$, $r_1 = 7$, $r_2 = 0.2$, $D_{u1} = D_{v1} = 0.5$, $D_{u2} = D_{v2} = 0.5$, $\mu_{u1} = \mu_{v1} = 1$, $\mu_{u2} = \mu_{v2} = 2$, $m_1 = m_2 = 1$

The dependence of the traveling wave speed on the preference parameters $\alpha_{u,v}$ is more complicated and differs significantly from the case of unstructured populations, see Fig. 4. When both age groups have the same preference for good patches (dotted curve), then the speed is a hump-shaped function: when preference for good patches is weak, individuals remain in bad patches and the population declines or spreads only slowly. When preference for good patches is very strong, individuals do not leave good patches so that the population spreads only slowly or not at all. This behavior is the same as in the unstructured model (Maciel and Lutscher 2013).

If, however, only one of the two age groups shows habitat preference whereas the other is neutral then the speed does not decrease to zero as preference approaches unity (dashed and dash-dot curve in Fig. 4). In fact, the two curves indicate that speed increases over almost the entire range of habitat preference. Details will depend

on parameters chosen. There is, however, an intuitive biological explanation for the observed pattern: A population with two stages could rely on only one stage for dispersal while reducing dispersal loss by high habitat preference in the other stage. In fact, many marine species have sessile adult populations and disperse only through the larval stage. We return to such a scenario in Sect. 8.

6 Wave speed in a homogeneous landscape

While the dispersion relation in a heterogeneous landscape is given only implicitly, we can use it to obtain the dispersion relation for a homogeneous landscape explicitly as a special case. Indeed, substituting $L_2 = 0$ into Eqs. (67)–(74) and equating the determinant of the coefficient matrix to zero, we arrive at the relation

$$(z_1^2 + z_2^2)^2(z_3^2 - z_4^2)^2 \left(1 + e^{2sL_1} - 2e^{sL_1} \cos(L_1z_1)\right) \left(1 + e^{2sL_1} - 2e^{sL_1} \cosh(L_1z_2)\right) = 0. \tag{75}$$

Since $z_1^2 + z_2^2 \neq 0$ and $z_3 \neq z_4$, this condition becomes

$$\left(1 + e^{2sL_1} - 2e^{sL_1} \cos(L_1z_1)\right) \left(1 + e^{2sL_1} - 2e^{sL_1} \cosh(L_1z_2)\right) = 0.$$

Dividing by $2e^{sL_1}$ gives

$$(\cosh(sL_1) - \cos(L_1z_1))(\cosh(sL_1) - \cosh(L_1z_2)) = 0.$$

Since we need $L_1 \neq 0$, we eventually find the condition $\cosh(sL_1) - \cosh(L_1z_2) = 0$, which has the solution $s = z_2$.

The dispersion relation for the spread speed in a homogeneously good landscape is therefore implicitly given by

$$s = \frac{1}{\sqrt{2D_{u_1}D_{v_1}}} \sqrt{D_{v_1}(m_1 + sC + \mu_{u_1}) + D_{u_1}(sC + \mu_{v_1}) + \Delta_1}, \tag{76}$$

where

$$\Delta_1 = \sqrt{[D_{v_1}(m_1 + sC + \mu_{u_1}) - D_{u_1}(sC + \mu_{v_1})]^2 + 4D_{u_1}D_{v_1}r_1m_1}.$$

We can solve (76) for C algebraically to give the following quadratic equation

$$0 = C^2 + C \left(\frac{\mu_{v_1} + \mu_{u_1} + m_1}{s} - sD_{u_1} - sD_{v_1} \right) + s^2D_{u_1}D_{v_1} - D_{v_1}m_1 - D_{v_1}\mu_{u_1} - D_{u_1}\mu_{v_1} + \frac{m_1\mu_{v_1} + \mu_{u_1}\mu_{v_1} - r_1m_1}{s^2}. \tag{77}$$

Accordingly, we obtain the two roots

$$\frac{1}{2s} \left((D_{u_1} + D_{v_1})s^2 - m_1 - \mu_{u_1} - \mu_{v_1} \pm \sqrt{4r_1m_1 + ((D_{u_1} - D_{v_1})s^2 - m_1 - \mu_{u_1} + \mu_{v_1})^2} \right). \tag{78}$$

Clearly, the expression with the ‘+’ in front of the root is larger than with the ‘-’. We show that the former has a global minimum for $0 < s < \infty$ whereas the latter does not.

We begin with the inequality for good patches (8), namely $r_1 > \frac{\mu_{v_1}}{m_1} (m_1 + \mu_{u_1})$. With this, we find

$$\begin{aligned} & \left(-m_1 - \mu_{u_1} - \mu_{v_1} + \sqrt{4r_1m_1 + (-m_1 - \mu_{u_1} + \mu_{v_1})^2} \right) \\ & > \left(-m_1 - \mu_{u_1} - \mu_{v_1} + \sqrt{4\mu_{v_1} (m_1 + \mu_{u_1}) + (-m_1 - \mu_{u_1} + \mu_{v_1})^2} \right) \\ & = \left(-m_1 - \mu_{u_1} - \mu_{v_1} + \sqrt{(m_1 + \mu_{u_1} + \mu_{v_1})^2} \right) = 0. \end{aligned}$$

Since the expression in large brackets in (78) is positive for $s = 0$ and increasing in s , we can calculate the limit

$$\begin{aligned} & \lim_{s \rightarrow 0^+} \frac{1}{2s} \left((D_{u_1} + D_{v_1})s^2 - m_1 - \mu_{u_1} - \mu_{v_1} \right. \\ & \quad \left. + \sqrt{4r_1m_1 + ((D_{u_1} - D_{v_1})s^2 - m_1 - \mu_{u_1} + \mu_{v_1})^2} \right) \\ & \geq \left(-m_1 - \mu_{u_1} - \mu_{v_1} + \sqrt{4r_1m_1 + (-m_1 - \mu_{u_1} + \mu_{v_1})^2} \right) \lim_{s \rightarrow 0^+} \left(\frac{1}{2s} \right) = \infty. \end{aligned} \tag{79}$$

Similarly, we obtain the limit for large s via

$$\begin{aligned} & \lim_{s \rightarrow \infty} \frac{1}{2s} \left((D_{u_1} + D_{v_1})s^2 - m_1 - \mu_{u_1} - \mu_{v_1} \right. \\ & \quad \left. + \sqrt{4r_1m_1 + ((D_{u_1} - D_{v_1})s^2 - m_1 - \mu_{u_1} + \mu_{v_1})^2} \right) \\ & = \lim_{s \rightarrow \infty} \frac{s}{2} \left(D_{u_1} + D_{v_1} + \frac{-m_1 - \mu_{u_1} - \mu_{v_1}}{s^2} \right. \\ & \quad \left. + \frac{\sqrt{4r_1m_1 + ((D_{u_1} - D_{v_1})s^2 - m_1 - \mu_{u_1} + \mu_{v_1})^2}}{s^2} \right) \\ & = \left(D_{u_1} + D_{v_1} + \sqrt{(D_{u_1} - D_{v_1})^2} \right) \lim_{s \rightarrow \infty} \left(\frac{s}{2} \right) = \infty. \end{aligned}$$

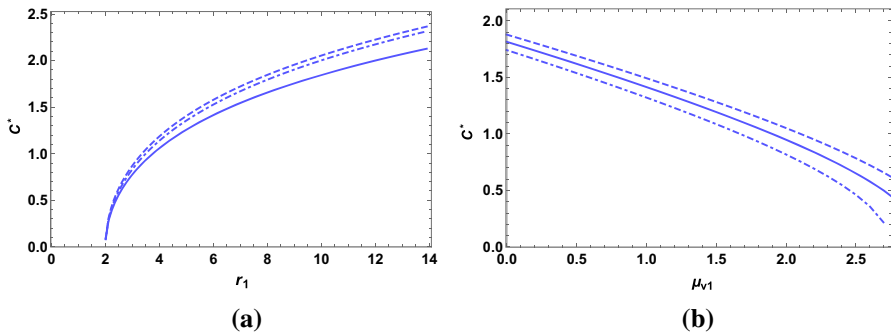


Fig. 5 Spread speed for the juveniles-adults model in a homogeneous landscape according to (80). **a** C^* as a function of reproduction rate r_1 with diffusion coefficients $D_{v_1} = 0.7$ (dashed), or $D_{u_1} = 0.7$ (dash-dot). The solid curve has default parameters $D_{u_1} = D_{v_1} = 0.5$. **b** C^* as a function of μ_{v_1} for maturation rate $m_1 = 1.15$ (dashed), $m_1 = 1$ (solid), and $m_1 = 0.85$ (dash-dot). Other parameters are as follows $r_1 = 6$, $\mu_{u_1} = 1$, and $\mu_{v_1} = 1$

Since the expression is continuous on $(0, \infty)$ and approaches infinity at either end, it must have a global minimum.

Similar calculations in the case with ‘-’ show that the limit for $s \rightarrow \infty$ is still infinity but the limit $s \rightarrow 0^+$ is negative infinity. Hence, there is no global minimum.

Proposition 6 *The dispersion relation for the homogeneously good landscape is given explicitly by*

$$C(s) = \frac{1}{2s} \left((D_{u_1} + D_{v_1})s^2 - m_1 - \mu_{u_1} - \mu_{v_1} + \sqrt{4r_1m_1 + ((D_{u_1} - D_{v_1})s^2 - m_1 - \mu_{u_1} + \mu_{v_1})^2} \right) \tag{80}$$

We cannot obtain an explicit expression for the minimum value C^* but we compute it numerically. As expected, the spread speed is an increasing function of growth rate; see Fig. 5a. This plot also shows that the spread speed is more sensitive to increasing adult diffusion than juvenile diffusion for this set of parameters. Similarly, the spread speed decreases as a function of adult mortality but increases with maturation rate; see Fig. 5b.

We can also use the explicit expression for the dispersion relation to obtain formulas for the sensitivity and elasticity of C^* with respect to population parameters. If p is any of the model parameters, we can differentiate the expression

$$C^*(p) = \min_{s>0} C(s, p) = C(s^*(p), p) \tag{81}$$

according to the chain rule and obtain

$$\frac{\partial C^*}{\partial p} = \left(\frac{\partial C}{\partial s} \cdot \frac{\partial s}{\partial p} \right) + \frac{\partial C}{\partial p} = \frac{\partial C}{\partial p}. \tag{82}$$

Table 2 Sensitivity and elasticity of the spread speed (C^*) with respect to default parameters: $D_{u_1} = D_{v_1} = 1, \mu_{u_1} = \mu_{v_1} = 1, r_1 = 6$ and $m_1 = 1$

Population parameter	Sensitivity value	Elasticity value
reproduction rate in patch type 1 (r_1)	0.2	0.6
maturation rate in patch type 1 (m_1)	0.8	0.4
juveniles diffusion term in patch type 1 (D_{u_1})	0.4	0.2
adults diffusion term in patch type 1 (D_{v_1})	0.6	0.3
juveniles mortality term in patch type 1 (μ_{u_1})	-0.4	-0.2
adults mortality term in patch type 1 (μ_{v_1})	-0.6	-0.3

The last equality holds since all derivatives are evaluated at $s = s^*$, where $\partial C / \partial s = 0$
 The sensitivities are given as follows

$$\frac{\partial C^*}{\partial r_1} = \frac{m_1}{s\sqrt{4r_1m_1 + (D_{u_1}s^2 - m_1 - D_{v_1}s^2 - \mu_{u_1} + \mu_{v_1})^2}}, \tag{83}$$

$$\frac{\partial C^*}{\partial m_1} = \frac{-1}{2s} + \frac{2r_1 - (D_{u_1}s^2 - m_1 - D_{v_1}s^2 - \mu_{u_1} + \mu_{v_1})}{2s\sqrt{4r_1m_1 + (D_{u_1}s^2 - m_1 - D_{v_1}s^2 - \mu_{u_1} + \mu_{v_1})^2}}, \tag{84}$$

$$\frac{\partial C^*}{\partial D_{u_1}} = \frac{s}{2}(1 + \sigma), \quad \frac{\partial C^*}{\partial D_{v_1}} = \frac{s}{2}(1 + \sigma), \tag{85}$$

$$\frac{\partial C^*}{\partial \mu_{u_1}} = \frac{-1}{2s}(1 + \sigma), \quad \frac{\partial C^*}{\partial \mu_{v_1}} = \frac{-1}{2s}(1 - \sigma), \tag{86}$$

with

$$\sigma = \frac{D_{u_1}s^2 - m_1 - D_{v_1}s^2 - \mu_{u_1} + \mu_{v_1}}{\sqrt{4r_1m_1 + (D_{u_1}s^2 - m_1 - D_{v_1}s^2 - \mu_{u_1} + \mu_{v_1})^2}}.$$

Since $|\sigma| < 1$, we conclude that the sensitivities in (85) are positive and those in (86) are negative. Clearly, the sensitivity with respect to r_1 in (83) is positive. The sign of the expression in (84) is unclear. In fact, we will see in Sect. 9 that it could have either sign. We present the numerical values of the sensitivities with respect to our default parameters in Table 2. We see that the sensitivity of C^* with respect to D_{v_1} is higher than sensitivity with respect to D_{u_1} .

7 Homogenization of the heterogeneous landscape

The explicit formulas for spread speeds in the previous section motivate us to apply homogenization techniques to the heterogeneous landscape and then use the above formulas for the resulting homogenized equations. Homogenization techniques have been applied to partial differential equations with Fickian diffusion terms (Othmer

1983) and with ecological diffusion (Garlick et al. 2011, 2014) in order to determine the impact of small scale habitat variation on large scale movement, and to explore the asymptotic spread speed. The discontinuities in the density functions in our equations pose an additional challenge for homogenization. Recently, Yurk and Cobbold (2018) solved the problem for a scalar equation. We extended their derivations to the case of structured populations. Since the calculations are rather lengthy but essentially the same as in the work by Yurk and Cobbold (2018), we only give the results here. Details can be found in the work by Alqawasmeh (2017). We then compare numerically the speeds for the homogenized equations and the dispersion relation from the previous section.

As before, we consider Eqs. (4, 5) in a periodically alternating landscape of good and bad patches of length L_1 and L_2 , respectively. We choose the period $\epsilon = L = L_1 + L_2 \ll 1$ as our small scale and introduce $y = x/\epsilon$ as a new variable. Then we write the density functions as functions of the large and small scale variables and expand in a formal power series in ϵ , i.e.

$$u(t, x, y) = u^{(0)}(t, x, y) + \epsilon u^{(1)}(t, x, y) + \epsilon^2 u^{(2)}(t, x, y) + \dots, \tag{87}$$

and similarly for v . We introduce the periodic step functions

$$h(y) = \begin{cases} 1, & \text{if } y \text{ is in good patch,} \\ k_u, & \text{if } y \text{ is in bad patch,} \end{cases} \quad \text{and} \quad \tilde{h}(y) = \begin{cases} 1, & \text{if } y \text{ is in good patch,} \\ k_v, & \text{if } y \text{ is in bad patch.} \end{cases}$$

We find that the lowest-order terms of u and v are given by

$$u^{(0)}(t, x, y) = \frac{\bar{u}(t, x)}{h(y)}, \quad v^{(0)}(t, x, y) = \frac{\bar{v}(t, x)}{\tilde{h}(y)}, \tag{88}$$

where functions \bar{u}, \bar{v} satisfy a system of reaction–diffusion equations on an appropriately homogenized landscape, namely

$$\frac{\partial \bar{u}}{\partial t} = \langle D \rangle_H (\widehat{L})^2 \frac{\partial^2 \bar{u}}{\partial x^2} + \langle f \rangle_A, \tag{89}$$

$$\frac{\partial \bar{v}}{\partial t} = \langle \tilde{D} \rangle_H (\widehat{\tilde{L}})^2 \frac{\partial^2 \bar{v}}{\partial x^2} + \langle \tilde{f} \rangle_A. \tag{90}$$

The harmonic mean of the diffusion coefficients and the rescaled length are given by

$$\langle D \rangle_H = \left(\frac{L_1 + \frac{L_2}{k_u}}{\frac{L_1}{D_{u_1}} + \frac{L_2}{D_{u_2}}} \right), \quad \text{and} \quad \widehat{L} = \left(\frac{L_1 + L_2}{L_1 + \frac{L_2}{k_u}} \right).$$

The corresponding expressions in the equation for \bar{v} have k_u replaced by k_v and D_{u_i} by D_{v_i} . The arithmetic averages of the reaction terms from (6, 7) are given by

$$\begin{aligned} \langle f \rangle_A &= \frac{L_1 f_{u1}(\bar{u}, \bar{v}) + L_2 f_{u2} \left(\frac{\bar{u}}{k_u}, \frac{\bar{v}}{k_v} \right)}{L_1 + \frac{L_2}{k_u}} \\ &= \frac{\left(L_1 r_1 + \frac{L_2 r_2}{k_v} \right) \bar{v} - \left(L_1 (\mu_{u1} + m_1) + \frac{L_2}{k_u} (\mu_{u2} + m_2) \right) \bar{u}}{L_1 + \frac{L_2}{k_u}}, \end{aligned}$$

and similarly for $\langle \tilde{f} \rangle_A$ in the equation for \bar{v} as

$$\begin{aligned} \langle \tilde{f} \rangle_A &= \frac{L_1 f_{v1}(\bar{u}, \bar{v}) + L_2 f_{v2} \left(\frac{\bar{u}}{k_u}, \frac{\bar{v}}{k_v} \right)}{L_1 + \frac{L_2}{k_u}} \\ &= \frac{\left(L_1 m_1 + \frac{L_2 m_2}{k_u} \right) \bar{u} - \left(L_1 \mu_{v1} + \frac{L_2 \mu_{v2}}{k_v} \right) \bar{v}}{L_1 + \frac{L_2}{k_v}}. \end{aligned}$$

System (89, 90) is a linear, cooperative system to which we can apply the theory developed in by Lui (1989); Zhao (2009). Specifically, the minimal traveling wave speed for this system is given by

$$C^* = \inf_{s>0} \frac{\lambda_1(s)}{s} \tag{91}$$

where $\lambda_1(s)$ is the dominant eigenvalue of the matrix

$$C_s = \begin{bmatrix} s^2 \langle D \rangle_H (\widehat{L})^2 - a & b \\ c & s^2 \langle \tilde{D} \rangle_H (\widehat{L})^2 - d \end{bmatrix}, \tag{92}$$

with

$$\begin{aligned} a &= \frac{L_1 (\mu_{u1} + m_1) + \frac{L_2}{k_u} (\mu_{u2} + m_2)}{L_1 + \frac{L_2}{k_u}}, & b &= \frac{L_1 r_1 + \frac{L_2 r_2}{k_v}}{L_1 + \frac{L_2}{k_u}}, \\ c &= \frac{L_1 m_1 + \frac{L_2 m_2}{k_u}}{L_1 + \frac{L_2}{k_v}}, & \text{and } d &= \frac{L_1 \mu_{v1} + \frac{L_2 \mu_{v2}}{k_v}}{L_1 + \frac{L_2}{k_v}}. \end{aligned}$$

We remark that the two expressions that we calculated for the dispersion relation in Eq. (78) correspond to the dominant and the subdominant eigenvalue of C_s above.

We illustrate the power of the homogenization method by comparing the dispersion relation (Fig. 6) and the resulting minimal wave speeds (Fig. 7) for the approximation and the exact expression. In all cases, we find an excellent agreement between the fully heterogeneous speed (from Proposition 5) and the homogenized speed (from Formula (91)), even though the landscape period is not of order ϵ the formal derivation requires.

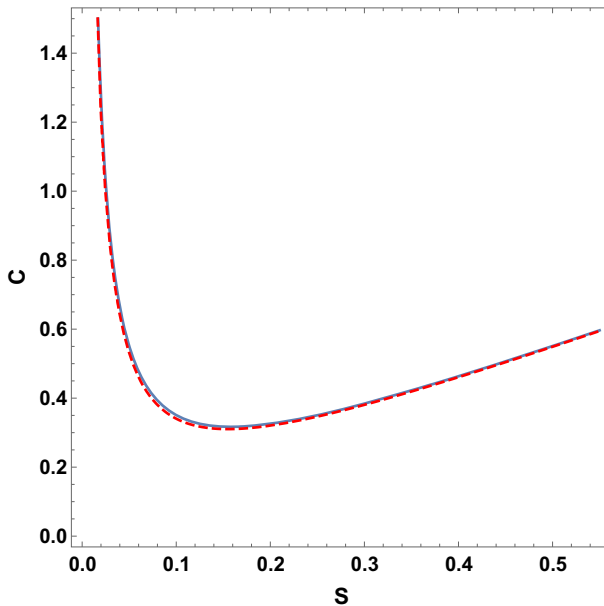


Fig. 6 Comparing the dispersion relation from the homogenization formula (91) (dashed curve) and the exact formula from Proposition 5 (solid). The two curves are virtually indistinguishable. Parameters are as follows: $L_1 = L_2 = 0.5$, $r_1 = 2.8$, $r_2 = 0.2$, $D_{u_1} = D_{v_1} = 0.6$, $D_{u_2} = D_{v_2} = 2$, $\mu_{u_1} = \mu_{v_1} = 0.9$, $\mu_{u_2} = \mu_{v_2} = 1$, $m_1 = m_2 = 1$, and $k_u = k_v = \frac{1}{\sqrt{0.3}}$

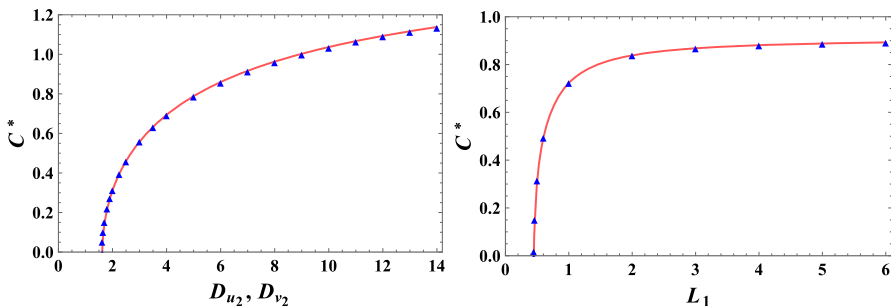


Fig. 7 Spread speed for the juvenile-adult model: **a** as a function of diffusion coefficients in bad patches; **b** as a function of good patch size. The solid curves corresponds to the homogenization formula (91), while the triangles refer to the spread speeds from the exact expression in Proposition 5. Unless otherwise noted, parameter values are as in the previous figure

8 Structured population with sessile adults

So far, we assumed that individuals of both age groups are mobile. Many organisms, however, have a life cycle with sessile adults. For example, many marine invertebrates are immobile as adults and release large numbers of larvae into the water column, where they are transported with the flow until they settle and mature. This scenario is represented by setting the diffusion coefficients in the equations for the adult popu-

lation to zero. Since the diffusion coefficients appear in the highest-order derivatives, we obtain a singular problem, and it is not clear that we can derive the corresponding persistence conditions and spread rates from the existing formulas by setting the diffusion coefficients in results equal to zero. Even if we could, some of the expressions are so complicated that it is not easy to see what the results would be. Instead, we illustrate how the calculations above carry over, and sometimes simplify significantly in that case.

8.1 Persistence conditions for a single patch

On a single good patch $x \in [0, L]$, the equations with sessile adults read

$$\frac{\partial}{\partial t} u = D_u \frac{\partial^2 u}{\partial x^2} + r v - (m + \mu_u) u \tag{93}$$

$$\frac{\partial}{\partial t} v = m u - \mu_v v, \tag{94}$$

with hostile boundary conditions $u(t, 0) = u(t, L) = 0$.

The corresponding eigenvalue problem to determine stability of the trivial solution is

$$\lambda U = D_u U'' - (m + \mu_u) U + r V, \tag{95}$$

$$\lambda V = m U - \mu_v V. \tag{96}$$

We solve (95) for V and substitute into (96) to get the second-order equation

$$U'' = \frac{1}{D_u} \left(\lambda - \frac{r m}{\lambda + \mu_v} + m + \mu_u \right) U. \tag{97}$$

To find the persistence boundary, we set $\lambda = 0$ and note that, according to the definition of a good patch in (8), we have the inequality $\left(-\frac{r m}{\mu_v} + m + \mu_u \right) < 0$. Then we obtain the solution of (97) as

$$U(x) = A \cos(q_1 x) + B \sin(q_1 x), \quad \text{with } q_1 = \sqrt{\frac{1}{D_u} \left(\frac{r m}{\mu_v} - m - \mu_u \right)}. \tag{98}$$

The hostile boundary conditions require $A = 0$ and $\sin(q_1 L) = 0$.

Proposition 7 *The critical patch size formula of model (93, 94) with hostile boundary is given by*

$$L^* = \pi \sqrt{\frac{D_u}{\frac{r m}{\mu_v} - m - \mu_u}}. \tag{99}$$

8.2 Persistence conditions for periodically varying landscapes

In a periodic landscape of two patch types, we have good patches of length L_1 with equations

$$\frac{\partial}{\partial t} u_1 = D_{u_1} \frac{\partial^2 u_1}{\partial x^2} + r_1 v_1 - (m_1 + \mu_{u_1}) u_1 \quad (100)$$

$$\frac{\partial}{\partial t} v_1 = m_1 u_1 - \mu_{v_1} v_1, \quad (101)$$

for $x \in (-L_1/2, L_1/2) + L\mathbb{Z}$ and the same equations with indices numbered '2' instead of '1' in bad patches of length L_2 . As before, it is sufficient to study the persistence problem, i.e. the corresponding eigenvalue problem, on half of one period, namely on $x \in [0, L/2]$. By symmetry on the unbounded domain, we have the boundary conditions

$$\frac{\partial u_1}{\partial x}(t, 0) = 0 = \frac{\partial u_2}{\partial x}(t, L/2). \quad (102)$$

At the interface $x = L_1/2$ we have the matching conditions

$$u_1 \left(t, \frac{L_1^-}{2} \right) = k_u u_2 \left(t, \frac{L_1^+}{2} \right), \quad (103)$$

and

$$D_{u_1} \frac{\partial u_1}{\partial x} \left(t, \frac{L_1^-}{2} \right) = D_{u_2} \frac{\partial u_2}{\partial x} \left(t, \frac{L_1^+}{2} \right), \quad (104)$$

As before, we look for exponential solutions in time which lead us to an eigenvalue problem in space. On the good patch $[0, L_1/2]$ this reads

$$\lambda U_1 = D_{u_1} U_1'' + r_1 V_1 - (m_1 + \mu_{u_1}) U_1, \quad (105)$$

$$\lambda V_1 = m_1 U_1 - \mu_{v_1} V_1, \quad (106)$$

and on the bad patch, the indices '1' are replaced by '2'. We solve the equations for V_i and substitute into the equations for U_i to get to the pair of second-order equations

$$\frac{d^2 U_1}{dx^2} = \frac{1}{D_{u_1}} \left(\lambda - \frac{r_1 m_1}{\lambda + \mu_{v_1}} + m_1 + \mu_{u_1} \right) U_1, \quad x \in \left(0, \frac{L_1}{2} \right), \quad (107)$$

and

$$\frac{d^2 U_2}{dx^2} = \frac{1}{D_{u_2}} \left(\lambda - \frac{r_2 m_2}{\lambda + \mu_{v_2}} + m_2 + \mu_{u_2} \right) U_2, \quad x \in \left(\frac{L_1}{2}, \frac{L}{2} \right). \quad (108)$$

In view of the boundary conditions, the general solutions can be written in the form

$$U_1(x) = A \cos(q_1 x), \quad U_2(x) = A' \cosh \left(q_2 \left(\frac{L}{2} - x \right) \right), \quad (109)$$

where

$$q_1 = \sqrt{\frac{1}{D_{u_1}} \left(\frac{r_1 m_1}{\mu_{v_1}} - m_1 - \mu_{u_1} \right)}, \quad q_2 = \sqrt{\frac{1}{D_{u_2}} \left(-\frac{r_2 m_2}{\mu_{v_2}} + m_2 + \mu_{u_2} \right)}. \tag{110}$$

Applying the interface conditions in (103) and (104) gives the linear equations

$$A \cos \left(q_1 \frac{L_1}{2} \right) - A' k_u \cosh \left(q_2 \frac{L_2}{2} \right) = 0, \tag{111}$$

and

$$A q_1 \sin \left(q_1 \frac{L_1}{2} \right) - A' q_2 D_u \sinh \left(q_2 \frac{L_2}{2} \right) = 0, \tag{112}$$

where $D_u = \frac{D_{u_2}}{D_{u_1}}$. This system has a non-trivial solution if and only if the determinant of the coefficient matrix

$$\begin{bmatrix} \cos \left(q_1 \frac{L_1}{2} \right) & -k_u \cosh \left(q_2 \frac{L_2}{2} \right) \\ q_1 \sin \left(q_1 \frac{L_1}{2} \right) & -q_2 D_u \sinh \left(q_2 \frac{L_2}{2} \right) \end{bmatrix} \tag{113}$$

is equal to zero.

Proposition 8 *The persistence boundary of model (100, 101) with interface conditions (103, 104) is given implicitly by*

$$D_u q_2 \tanh \left(q_2 \frac{L_2}{2} \right) = k_u q_1 \tan \left(q_1 \frac{L_1}{2} \right), \tag{114}$$

where q_i are defined in (110).

We compare the minimal size of a good patch, L_1^* , from (114) with the limiting case of very low mobility in the general formula (44). We observe that, as the diffusion rates for adults in (44) approach zero, the minimal good patch size approaches that of formula (114). When adults are mobile, larger good patches are required for population persistence since mobile adults may leave good patches and enter bad patches (Fig. 8). As adults' preference for good habitat increases, the size requirement for good patches decreases.

8.3 Traveling wave speed in heterogeneous landscapes

Finally, we find the dispersion relation to obtain the minimal traveling periodic wave speed in the case of sessile adults. For a TPW of speed $C > 0$ to the right, we make the same ansatz as in (45) with $z = x - Ct$ and find the same form as in (46), namely

$$u(t, x) = e^{-sz} g(x), \quad v(t, x) = e^{-sz} \tilde{g}(x). \tag{115}$$

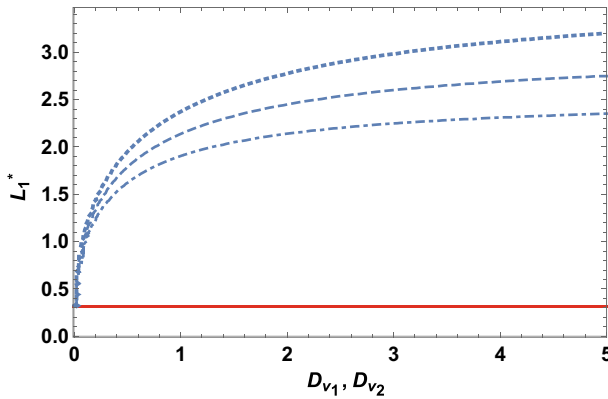


Fig. 8 Minimal good patch size for a structured population of juveniles and adults, L_1^* , as a function of adults' diffusion rate ($D_{v_1} = D_{v_2}$) according to (44). The three curves correspond to adults' habitat preference $\alpha_v = 0.45$ (dotted), $\alpha_v = 0.5$ (dashed), and $\alpha_v = 0.55$ (dash-dot). The solid line represents the critical good patch size in the case of sessile adults according to (114). Other parameters are as follows: $r_1 = 2, r_2 = 0.2, \mu_{u_1} = \mu_{v_1} = 1, \mu_{u_2} = \mu_{v_2} = 2, m_1 = 5, m_2 = 1, D_{u_1} = 1, D_{u_2} = 2, \alpha_u = 0.5$, and $L_2 = 1$

As before, we write $g = g_{1,2}$ and $\tilde{g} = \tilde{g}_{1,2}$ on good and bad patches, respectively. What follows is very similar to the calculations in Sect. 5 but simpler. We give only the most important steps.

Substituting the expressions in (115) into Eqs. (100, 101) on good patches, we obtain the system

$$sCg_1(x) = D_{u_1} \left(s^2g_1(x) + g_1''(x) - 2sg_1'(x) \right) + r_1\tilde{g}_1(x) - (m_1 + \mu_{u_1})g_1(x), \tag{116}$$

$$sC\tilde{g}_1(x) = m_1g_1(x) - \mu_{v_1}\tilde{g}_1(x). \tag{117}$$

We solve the latter equation for \tilde{g}_1 and substitute the expression into the former. Then we sort by derivatives of g_1 and get

$$g_1''(x) - 2sg_1'(x) + \frac{1}{D_{u_1}} \left(D_{u_1}s^2 + \frac{r_1m_1}{sC + \mu_{v_1}} - m_1 - \mu_{u_1} - sC \right) g_1(x) = 0. \tag{118}$$

The characteristic equation for (118) has the two roots

$$z = s \pm q_1 := s \pm \frac{1}{\sqrt{D_{u_1}}} \sqrt{m_1 + sC + \mu_{u_1} - \frac{r_1m_1}{sC + \mu_{v_1}}}. \tag{119}$$

The solution of the differential equation in (118) is of the form

$$g_1(x) = e^{sx} [A \cosh(q_1x) + B \sinh(q_1x)]. \tag{120}$$

The same procedure applied on bad patches gives the differential equation for g_2 as

$$g_2''(x) - 2s g_2'(x) + \frac{1}{D_{u_2}} \left(D_{u_2} s^2 + \frac{r_2 m_2}{sC + \mu_{v_2}} - m_2 - \mu_{u_2} - sC \right) g_2(x) = 0, \tag{121}$$

which has the corresponding solution

$$g_2(x) = e^{sx} [A' \cosh(q_2 x) + B' \sinh(q_2 x)], \tag{122}$$

where $q_2 = \frac{1}{\sqrt{D_{u_2}}} \sqrt{m_2 + sC + \mu_{u_2} - \frac{r_2 m_2}{sC + \mu_{v_2}}}$.

The four interface conditions

$$g_1(0^+) = k_u g_2(0^-), \quad g_1(L_1^-) = k_u g_2(-L_2^+), \tag{123}$$

$$g_1'(0^+) - s g_1(0^+) = D_u [g_2'(0^-) - s g_2(0^-)], \tag{124}$$

and

$$g_1'(L_1^-) - s g_1(L_1^-) = D_u [g_2'(-L_2^+) - s g_2(-L_2^+)]. \tag{125}$$

give linear relations between the four coefficients A, A', B, B' . The corresponding coefficient matrix turns out to be

$$\begin{bmatrix} 1 & 0 & -k_u & 0 \\ e^{sL} \cosh(q_1 L_1) & e^{sL} \sinh(q_1 L_1) & -k_u \cosh(q_2 L_2) & k_u \sinh(q_2 L_2) \\ 0 & q_1 & 0 & -D_u q_2 \\ q_1 e^{sL} \sinh(q_1 L_1) & q_1 e^{sL} \cosh(q_1 L_1) & q_2 D_u \sinh(q_2 L_2) & -q_2 D_u \cosh(q_2 L_2) \end{bmatrix}.$$

The linear system of equations has a nontrivial solution if and only if the determinant of this matrix is zero.

Proposition 9 *The dispersion relation for a TPW in a periodic alternating landscape and with sessile adult stage is given implicitly by*

$$\cosh(sL) = \cosh(q_1 L_1) \cosh(q_2 L_2) + \frac{(k_u q_1)^2 + (D_u q_2)^2}{2D_u k_u q_1 q_2} \sinh(q_1 L_1) \sinh(q_2 L_2). \tag{126}$$

We compare the minimal TPW speed calculated here with the minimal speed for the structured population from Proposition 5 in the limit of vanishing adult dispersal. Figure 9 shows that when adult mobility decreases to zero, the spread speed will approach the one from (126). Increasing adult mobility can decrease the population spread rate. This decrease indicates that the loss of individuals due to movement into bad patches has a strong negative impact; stronger than the positive impact that could be expected from having adults move and contribute to spread. If adults have a strong enough preference for good patches, then the population spread rate can eventually be higher with mobile than with sessile adults (dotted line in Fig. 9). But when adult

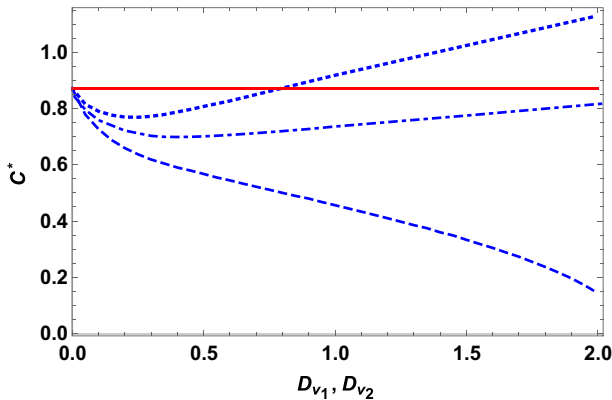


Fig. 9 Minimal traveling wave speed for a structured population of two age groups (see Proposition 5) as a function of adult mobility ($D_{v_1} = D_{v_2}$) with adult habitat preference at $\alpha_v = 0.55$ (dotted), $\alpha_v = 0.5$ (dash-dot), and $\alpha_v = 0.45$ (dashed). The straight line represents the minimal traveling wave speed with sessile adults according to (126). The remaining parameter values are $L_1 = 1, L_2 = 1, D_{u_1} = 0.5, D_{u_2} = 1, r_1 = 7, r_2 = 0.2, \mu_{u_1} = \mu_{v_1} = 1, \mu_{u_2} = \mu_{v_2} = 2, m_1 = m_2 = 1,$ and $\alpha_u = 0.5$

preference for good patches is low, increased adult dispersal can slow the invasion and eventually bring it to a halt. In this case, too many adults enter the bad patches and die there before they make it to the next nearest good patch. The effect that higher diffusion can lead to faster *or* slower population spread, depending on the strength of preference for good patches might also occur in the unstructured population model studied by Maciel and Lutscher (2013), but we are not aware of any previous mentioning. Clearly, a positive speed in the absence of diffusion (in one age group) is impossible in the unstructured model.

As before, we can derive a formula for the minimal wave speed in a homogeneous landscape. Substituting $L_2 = 0$ in the dispersion relation (126), we get

$$\cosh(sL_1) = \cosh(q_1L_1). \tag{127}$$

Following the same steps as previously, we eventually obtain the explicit dispersion relation

$$C(s) = \frac{1}{2s} \left(-m_1 - \mu_{u_1} - \mu_{v_1} + D_{u_1}s^2 + \sqrt{4r_1m_1 + (D_{u_1}s^2 - m_1 - \mu_{u_1} + \mu_{v_1})^2} \right). \tag{128}$$

It turns out that this expression is the same as when we set $D_{v_1} = 0$ in the wave speed formula for juveniles-adults model in homogeneous landscape (80).

9 The importance of maturation rate

We illustrate our results about persistence conditions and spread rates by focusing on the effect of the maturation rate. Specifically, we answer the question of when a simple,

unstructured population model is sufficient and when the more complex structured model that we studied here is required. Since the unstructured model assumes that individuals can reproduce immediately after being born, we expect that our model reduces to the unstructured model in the limit of high maturation rates. We begin by making this idea more precise.

We recall the non-spatial model

$$\dot{u} = rv - (m + \mu_u)u, \quad \dot{v} = mu - \mu_v v, \tag{129}$$

from (1) and the persistence condition $r > \mu_v \left(1 + \frac{\mu_u}{m}\right)$ from Proposition (1).

In the extreme case when $m \rightarrow 0$, the persistence condition will be violated. Juveniles die before they mature, and the population declines. On the other hand, when $m \rightarrow \infty$, the persistence condition reduces to $r > \mu_v$. The juvenile stage is so short that juvenile mortality becomes irrelevant.

In the limit of large m , we have $m + \mu_u \approx m$ so that we can add the equations for u and v and get

$$\frac{d}{dt}(u + v) \approx (r - \mu_v)v.$$

Dividing the equation for u by m , we find

$$\frac{\dot{u}}{m} = \frac{rv}{m} - \left(1 + \frac{\mu_u}{m}\right)u,$$

so that in the limit for large m , we formally find $u \approx 0$. Hence, in the limit for large m , we obtain the unstructured (linear) model

$$\dot{v} = (r - \mu_v)v,$$

which we will use for comparison with our structured model.

We begin with comparing the minimal domain-size for the structured model (11,12) with the unstructured model by Skellam (1951)

$$\frac{\partial v}{\partial t} = D_v \frac{\partial^2 v}{\partial x^2} + (r - \mu_v)v. \tag{130}$$

Taking the limit $m \rightarrow \infty$ in formula (22) gives

$$\lim_{m \rightarrow \infty} L^* = \lim_{m \rightarrow \infty} \frac{\pi}{z_2} = \pi \sqrt{\frac{D_v}{r - \mu_v}}, \tag{131}$$

which is exactly the formula derived by Skellam (1951).

We had already found that the minimal patch size increases when maturation rate decreases. As individuals spend more time in the juvenile stage, they risk mortality and loss from the domain by moving across the hostile boundary. The combined effect is a

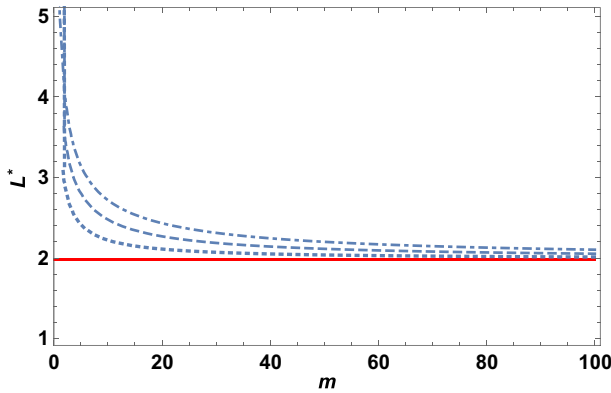


Fig. 10 Minimal patch size as a function of maturation coefficient according to formula (22) with juveniles diffusion coefficient $D_u = 2$ (dashed), $D_u = 4$ (dash-dot), and $D_u = 0.5$ (dotted). The solid line indicates the value from Skellam’s formula (131). Parameters are as follows: $\mu_u = \mu_v = 1$, $D_v = 2$, and $r = 6$

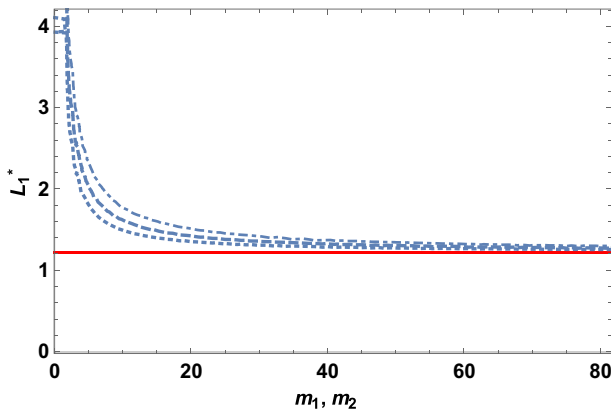


Fig. 11 Minimal size of good patches in a patchy periodic landscape as a function of maturation coefficients ($m_1 = m_2$) according to the structured populations persistence condition (44), with juveniles habitat preference $\alpha_u = 0.9$ (dotted), $\alpha_u = 0.5$ (dashed), and $\alpha_u = 0.1$ (dash-dot). The solid line indicates the value for the unstructured population (Equation 10 by Maciel and Lutscher 2013). Parameters are as follows: $D_{v_1} = D_{u_1} = 1$, $D_{v_2} = D_{u_2} = 2$, $\mu_{u_1} = \mu_{v_1} = 1$, $\mu_{v_2} = \mu_{u_2} = 2$, $L_2 = 2$, $\alpha_v = 0.5$, $r_1 = 2$, and $r_2 = 0.2$

larger area requirement for persistence. The critical size for the structured population decreases to the critical size for the unstructured population as maturation increases; see Fig. 10.

For a heterogeneous landscape consisting of two periodically alternating patch types, we compare our results for the structured population from Proposition (3) to the results for the unstructured population; see Equation (10) in the work by Maciel and Lutscher (2013). The implicit formula from Proposition (3) cannot simply be reduced by letting $m_1 \rightarrow \infty$. The numerical comparison in Fig. 11 shows that the critical size for a good patch according to (44) decreases to the critical size for the unstructured population.

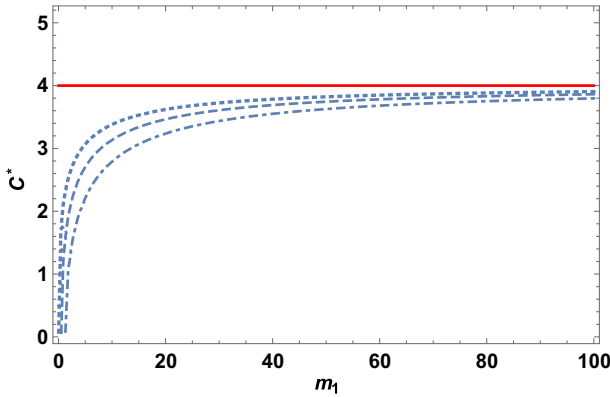


Fig. 12 Spread speed in a homogeneous landscape as a function of maturation coefficient according to the traveling wave speed formula (80), with juveniles mortality coefficient $\mu_{u_1} = 0.1$ (dotted), $\mu_{u_1} = 2$ (dashed), and $\mu_{u_1} = 5$ (dash-dot). The solid curve represents Fisher’s speed for the unstructured population model. Parameters are as follows: $D_{v_1} = D_{u_1} = 1$, $\mu_{v_1} = 1$, and $r_1 = 5$

For a comparison of the spreading speed between the structured and unstructured population, we begin with the homogeneous landscape. We find the limit as $m_1 \rightarrow \infty$ by rationalizing the numerator of the dispersion relation (80) to get

$$\begin{aligned} &\lim_{m_1 \rightarrow \infty} \frac{1}{2s} \left(D_{u_1} s^2 + D_{v_1} s^2 - m_1 - \mu_{u_1} - \mu_{v_1} + \sqrt{4r_1 m_1 + (D_{u_1} s^2 - m_1 - D_{v_1} s^2 - \mu_{u_1} + \mu_{v_1})^2} \right) \\ &= \lim_{m_1 \rightarrow \infty} \frac{1}{2s} \frac{-4(m_1 - D_{u_1} s^2 + \mu_{u_1})(D_{v_1} s^2 - \mu_{v_1}) - 4r_1 m_1}{D_{u_1} s^2 + D_{v_1} s^2 - m_1 - \mu_{u_1} - \mu_{v_1} - \sqrt{4r_1 m_1 + (D_{u_1} s^2 - m_1 - D_{v_1} s^2 - \mu_{u_1} + \mu_{v_1})^2}}. \end{aligned} \tag{132}$$

Dividing numerator and denominator in (132) by m_1 , we can evaluate the limit when $m_1 \rightarrow \infty$, as

$$\lim_{m_1 \rightarrow \infty} C(s) = \frac{r_1 - \mu_{v_1}}{s} + s D_{v_1}. \tag{133}$$

The minimum value of (133) occurs at $s = \sqrt{\frac{r_1 - \mu_{v_1}}{D_{v_1}}}$ and is given by

$$C^* = 2\sqrt{D_{v_1}(r_1 - \mu_{v_1})}. \tag{134}$$

This expression is exactly the spread speed for the unstructured population in (130) in a homogeneous landscape that was derived by Fisher (1937).

Figure 12 shows that the spread speed for a structured population in a homogeneous landscape is lower than the spread speed for the corresponding unstructured population. This result could be expected because in structured populations some juveniles die before they reproduce so that the overall population proceeds more slowly.

So far, we only observed a monotone relationship between the quantity of interest and the maturation rate. For the critical patch size, a monotone relationship seems intuitive since longer maturation times imply higher loss rates either through death or

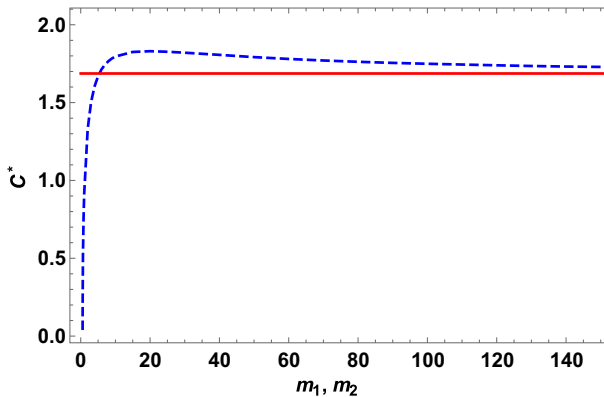


Fig. 13 Spread speed in a heterogeneous landscape as a function of maturation coefficients ($m_1 = m_2$). The dashed curve corresponds to the structured population, while the solid curve refers to unstructured population. Parameters are as follows: $L_1 = L_2 = 1$, $r_1 = 2.8$, $r_2 = 0.2$, $D_{u_1} = D_{v_1} = 0.6$, $\mu_{u_1} = \mu_{v_1} = 0.9$, $\mu_{u_2} = \mu_{v_2} = 1$, $D_{u_2} = 16$, $D_{v_2} = 1$, $\alpha_u = 0.2$, and $\alpha_v = 0.8$

through dispersal. In the context of spread rates, however, dispersal plays an ambivalent role: it increases loss when individuals move into bad patches, but it also increases spread rate since individuals move further/faster. To obtain a high spread rate, a population needs to grow well and move far. A structured population can divide these two tasks between the different stages. For example, adults could have a high preference for good patches and thereby ensure a high growth rate, while juveniles could have a high dispersal rate, thereby ensuring fast propagation.

Figure 13 shows that such a combination of parameters can indeed lead to spread rates at intermediate maturation rates being higher than at high maturation rates. The two curves are based on the implicit relation for the structured population (dashed) in Proposition 5 and from the corresponding dispersion relation (equation A32 by Maciel and Lutscher 2013) for the corresponding unstructured population (solid).

10 Discussion

Persistence of species, in particular rare species, and spatial spread of potentially invasive species have been two of the main concerns of ecological research for decades. A more recent aspect of special concern in this context is spatial heterogeneity, often induced by human activities. In strongly heterogeneous environments, the fate of a population is decided by how individuals use resources in space and avoid unfavorable regions.

Many species of ecological concern have complicated life cycles. For example, Blanding's turtle, a Canadian species at risk, takes 14–20 years to reach sexual maturity. Individuals at different life stages have vital rates (Cushing 1998; Singh and Krimbas 2000; Hastings and Gross 2012), different movement behaviors (Berger 1986; Stenseth and Lidicker 1992) and different habitat requirements. How then, would the interplay between stage-specific behavior and spatial heterogeneity affect population persistence and spatial spread?

Mathematical models continue to contribute insights and guidelines to the management of species at risk and invasive species. Questions about reserve design go back to the work by Skellam (1951) and Kierstead and Slobodkin (1953) on the minimal patch-size for a population, and have been extended and refined considerably since then Cantrell and Cosner (2003)). Questions about spatial spread go back to the seminal work by Fisher (1937) and Kolmogorov et al. (1937). Since the work by Aronson and Weinberger (1975) on the asymptotic spreading speed, the theory of spread speeds and traveling waves has been extended in many directions (Zhao 2009). More recently, building on the work by Shigesada et al. (1986), Maciel and Lutscher (2013) included individual behavior and began the exploration of how habitat preference and movement decisions affect population persistence and spatial spread. Our work here builds on their modeling framework and extends their work to structured populations.

We formulated a model for two life stages and two types of habitat. We analyzed persistence conditions in various habitat arrangements, and we derived the dispersion relation for the speed of a traveling periodic wave. We found that populations with very short maturation times can be well approximated by unstructured population models. Populations with longer maturation times, however, require larger habitats for persistence, all other factors being equal. The minimal traveling wave speed is not necessarily a monotone function of maturation rate. In particular, the spread rate of a structured population can be higher than that of a corresponding unstructured population if, for example, the juvenile stage has a high dispersal rate and the adult stage a high fidelity to source patches.

Our model formulation can be extended to more than two stages and to more than two patch types. The resulting calculations will be similar but much more tedious. In that context, the homogenization procedure will be particularly helpful. The recent progress on homogenization with discontinuous density function (Yurk and Cobbold 2018) that we extended here will clearly carry over to models with more stages and patch types or continuously varying landscape quality.

Our model formulation requires that stage duration is exponentially distributed. If this assumption is violated, then the discrete stages are typically replaced by a continuous stage structure, which usually leads to an integral formulation of the model and can sometimes be reduced to a delayed equation (Fang et al. 2014). While abstract results regarding stability and spread rates are available for these equations, we are unaware of any more explicit formulas in the spirit of what we derived here. Alternatively, one can introduce a larger number of (sub-)compartments and thereby model Γ -distributed stage durations. In this case, the modelling framework is the same as what we presented and all calculations are similar but—due to the larger number of stages—more tedious. This approach is closely related to integrodifference equation models as they were studied in homogeneous habitats by Lui (1989), Neubert and Caswell (2000) and others. The corresponding theory for patchy landscapes in integrodifference equations for unstructured populations was initiated by Musgrave and Lutscher (2014a, b). The corresponding theory for structured equations is still missing.

We consider only the linear model for population growth, death, and maturation. This model is only valid when densities are reasonably low; at high density, we expect nonlinear effects to arise. However, the linear model still provides us with most of the important information regarding persistence and spread rates, as long as the popula-

tion does not experience an Allee effect. The stage structure ensures that the system is cooperative so that the spreading speed of a nonlinear model (without Allee effect) in a homogeneous landscape is defined by the linearization at zero (Lui 1989; Zhao 2009). Hence the speed formulas in those cases give the asymptotic spreading speed. Extending the spreading speed theory to our model in a patchy landscape with discontinuous densities at interfaces remains an analytical challenge.

Acknowledgements We are grateful for inspiring discussions with Gabriel Maciel and Jeffrey Musgrave. We also thank Brian Yurk and Christina Cobbold to share their work on homogenization in the early stages of their work. Finally, we deeply thank two anonymous reviewers who pointed out the necessity for the eigenfunctions in Propositions 3 and 5 to be positive. We also thank editor Vincent Calvez for suggestions in the proof of Proposition 4.

Appendix

We give the proof of Proposition 4. The proof is split into several propositions. Several of these are extensions of Propositions 3.3 and 3.4 by Maciel et al. (submitted). We begin with the following observation.

The inverse of the matrix

$$M = \begin{bmatrix} \rho & -r \\ -m & \sigma \end{bmatrix} \tag{135}$$

is given by

$$M^{-1} = \frac{1}{\rho\sigma - rm} \begin{bmatrix} \sigma & r \\ m & \rho \end{bmatrix}. \tag{136}$$

In particular, if all parameters are positive and $\rho\sigma > rm$ then all solutions of $M \begin{bmatrix} u \\ v \end{bmatrix} = \begin{bmatrix} f \\ g \end{bmatrix}$ are non-negative provided $f, g \geq 0$.

We now consider the problem

$$-D_{u_i}u_i'' + \rho_i u_i - r_i v_i = f_i, \quad x \in \Omega_i, \tag{137}$$

$$-D_{v_i}v_i'' - m u_i + \sigma_i v_i = g_i, \quad x \in \Omega_i, \tag{138}$$

with $\Omega_1 = [0, l_1]$ and $\Omega_2 = [l_1, l_2]$. We assume that all parameters are positive and that $\rho_i \sigma_i > r_i m_i$ for $i = 1, 2$. Furthermore, we assume that $u_i' = v_i' = 0$ for $x = 0, l_2$ and that the interface conditions (9) and (10) hold at $x = l_1$.

Proposition 10 *Assume that u_i, v_i are twice continuously differentiable functions that satisfy (139) and (140) with boundary and interface conditions as indicated. If $f_i, g_i \geq 0$ then $u_i, v_i > 0$.*

Proof Suppose that u_1 or u_2 have a negative minimum, say, $u_1(x_1) < 0$. We distinguish two cases: x_1 can be an interior or a boundary point. If x_1 is an interior point, then $u_1''(x_1) \geq 0$. From (139), we find

$$0 > \rho_1 u_1(x_1) \geq f_1 + r_1 v_1(x_1),$$

which implies that $v_1(x_1) < 0$ as well. In particular, v_1 also has a negative minimum, say, $v_1(x_2) < 0$. There are again two cases to consider. If x_2 is in the interior, then we obtain

$$\sigma_1 v_1(x_2) - m_1 u_1(x_1) \geq \sigma_1 v_1(x_2) - m_1 u_1(x_2) \geq g_1(x_2) \geq 0.$$

Similarly, we find

$$\rho_1 u_1(x_1) - r_1 v_1(x_2) \geq \rho_1 u_1(x_1) - r_1 v_1(x_1) \geq f_1(x_1) \geq 0.$$

Then the preceding considerations about matrix M in (135) imply that $u_1(x_1), v_1(x_2) \geq 0$, which is a contradiction.

Next, we suppose that $x_2 = 0$. By the boundary condition, we have $v'_1(0) = 0$. If $v_1(x) \equiv v_1(0) < 0$ is a constant, then $\sigma_1 v_1 - m_1 u_1 = g_1 \geq 0$ in $(0, l_1)$ and the argument continues as above, which leads to a contradiction. If v_1 is not constant then there must be some point with $v_1(x) > v_1(0)$. Hence, there must be some point with $v'_1(x) > 0$ and therefore also some x_3 with $v''_1(x_3) > 0$. Since $v_1(0) < 0$ and v_1 is continuous, we can assume that $v_1(x_3) < 0$. Then again the same arguments as above lead to a contradiction.

Finally, we suppose that $x_2 = l_1$, the interface point. Since $v'_1(l_1)$ and $v'_2(l_1)$ have the same sign by the interface conditions, we necessarily have $v'_1(l_1) = 0$. Otherwise, it cannot be a minimum point. But then we are in the same case as previously when $x_2 = 0$. Hence, we have a contradiction again. We have shown that $u_{1,2}$ cannot have a negative minimum in the interior of Ω_i .

It remains to show that a negative minimum of $u_{1,2}$ cannot occur at a boundary or interface point either. We begin by assuming that $x_1 = 0$ is a negative minimum of u_1 . If u is constant, then we obtain the relation

$$\rho_1 u_1 - r_1 v_1 = f_1 \geq 0, \quad \text{in } \Omega_1,$$

which implies $v_1 < 0$ as well. Hence, v_1 has a negative minimum, which we can exclude by the same reasoning as above. If u_1 is not constant, then there is some region near $x = 0$, where u_1 is negative but larger than at the boundary point. Hence, there is a point where u'_1 is positive and then also where u''_1 is positive all the while u is negative. This brings us back to the situation from before, so that we obtain a contradiction again.

Finally, if $u_{1,2}$ assume a negative minimum at the interface point, i.e. $x_1 = l_1$, we first note that necessarily $u'_1(l_1) = u'_2(l_1) = 0$. Then we are in the same position as before when $x_1 = 0$, and we obtain a contradiction as before. Hence, u cannot have a negative minimum.

The same reasoning shows that $v_{1,2}$ cannot have a negative minimum either.

Finally, we assume that f_i and g_i are non-negative and that at least one of these functions is positive somewhere, say f_1 . Then u_1 satisfies the elliptic equation

$$-D_{u_1} u''_1 + \rho_1 u_1 = f_1 + r_1 v_1,$$

where the right-hand side is non-negative and not identically zero. By the strong maximum principle, we then get $u_1 > 0$ on Ω_1 . The strong maximum principle again then implies that $v_1 > 0$ on Ω_1 . Then $u_i(l_1), v_i(l_1) > 0$ and by the maximum principle, we also get $u_2, v_2 > 0$ on Ω_2 . \square

Proposition 11 *Suppose $\rho_i \sigma_i > r_i m_i$. For every $(f_1, g_1, f_2, g_2) \in \mathcal{C}(\Omega_1)^2 \times \mathcal{C}(\Omega_2)^2$ there exists a unique solution $(u_1, v_1, u_2, v_2) \in \mathcal{C}^2(\Omega_1)^2 \times \mathcal{C}^2(\Omega_2)^2$ of (139)–(140) with boundary and interface conditions as indicated, and*

$$\|(u_1, v_1, u_2, v_2)\|_{\mathcal{C}^2} \leq K \|(f_1, g_1, f_2, g_2)\|_{\mathcal{C}},$$

for some positive constant K , where the norm on the product spaces is simply the sum of the norms on each component.

Proof We first consider Eqs. (139)–(140) with Neumann boundary conditions on each interval. Hence, the equations on different intervals decouple. On each interval separately, the existence of solutions is guaranteed by standard existence theory for elliptic systems. At a maximum of u_1 , we have $u_1'' \leq 0$, so that we get

$$\rho_1 \|u_1\|_{\mathcal{C}} \leq \|f_1\|_{\mathcal{C}} + r_1 \|v_1\|_{\mathcal{C}}.$$

A similar estimate for $\|v_1\|_{\mathcal{C}}$ then gives

$$\rho_1 \|u_1\|_{\mathcal{C}} \leq \|f_1\|_{\mathcal{C}} + r_1 \|v_1\|_{\mathcal{C}} \leq \|f_1\|_{\mathcal{C}} + \frac{r}{\sigma_1} (g_1 + m_1 \|u_1\|_{\mathcal{C}}).$$

Hence, we find

$$(\rho_1 \sigma_1 - r_1 m_1) \|u_1\|_{\mathcal{C}} \leq \sigma_1 \|f_1\|_{\mathcal{C}} + r \|g_1\|_{\mathcal{C}}.$$

Since the factor in front of $\|u_1\|_{\mathcal{C}}$ is positive by assumption, we find an estimate of the form $\|u_1\|_{\mathcal{C}} \leq K_1 \|(f_1, g_1)\|_{\mathcal{C}}$. A similar estimate holds for $\|v_1\|_{\mathcal{C}}$.

With this estimate, we can bound the second derivative as

$$\|u_1''\|_{\mathcal{C}} = \|f_1 - \rho_1 u_1 + r_1 v_1\|_{\mathcal{C}} \leq K_2 \|(f_1, g_1)\|_{\mathcal{C}}.$$

Finally, we can bound the first derivative from the second by integration. Similar estimates hold for v_1 and also on Ω_2 . Hence, we have the desired estimate.

Next, we tend to the interface conditions. This step is exactly as in the proof of Proposition 3.4 by Maciel et al. (submitted). We consider the equation

$$-D_{u_1} y_1'' + \rho_1 y_1 = 0, \quad x \in \Omega_1,$$

with $y_1(0) = 1$ and $y_1'(0) = 0$. The solution satisfies $y_1(l_1) > 0$ and $y_1'(l_1) > 0$. Similarly, we consider

$$-D_{u_2} y_2'' + \rho_2 y_2 = 0, \quad x \in \Omega_2,$$

with $y_2(l_2) = 1$ and $y_2'(l_2) = 0$. Its solution satisfies $y_2(l_2) > 0$ and $y_2'(l_1) < 0$.

Then we define $\tilde{u}_i = u_i + a_i y_i$. By construction, \tilde{u}_i satisfy the differential equations for each a_i . By evaluating the interface conditions, we notice that we can choose a_i such that \tilde{u}_i also satisfy the interface conditions. The solutions depend on model parameters but not on functions f_i . Hence, by possibly adjusting the constant K , the norm estimate from above still holds for \tilde{u}_i . A similar construction applies to v_i . \square

Proposition 12 *Under the assumptions in the previous proposition, the operator defined by the left-hand sides in (139)–(140) with boundary and interface conditions as indicated has a principal eigenvalue with positive eigenfunction.*

Proof The proof follows from the previous two propositions in exactly the same way as the proof of Proposition 3.5 by Maciel et al. (submitted) by an application of the Krein-Rutman theorem (Du 2006). \square

Proof of Proposition 4 The eigenvalue problem studied in Sect. 4 can be written in the form

$$-D_{u_i} u_i'' + (\mu_{u_i} + m_i)u_i - r_i v_i = -\lambda u_i, \quad x \in \Omega_i, \quad (139)$$

$$-D_{v_i} v_i'' - m u_i + \mu_{v_i} v_i = -\lambda v_i, \quad x \in \Omega_i, \quad (140)$$

with $\Omega_1 = [0, L_1/2]$ and $\Omega_2 = [L_1/2, L - L_1/2]$. The boundary conditions are no-flux conditions at $x = 0$ and $x = L - L_1/2$ by symmetry (compare the reasoning leading up to Eq. 36). The interface conditions at $x = L_1/2$ are as in (9) and (10), or, explicitly in (38)–(39).

By the previous proposition, there is a principal eigenvalue, λ^* , with a positive eigenfunction. The population can persist if this eigenvalue is positive. For $L_1 = 0$ the entire domain is a ‘bad patch’ so that the principle eigenvalue is negative and the population cannot persist. Now let L^* be the smallest positive value of L such that (44) is satisfied, i.e. such that $\lambda = 0$ is an eigenvalue. If the corresponding eigenfunction is not of one sign then the principal eigenvalue, $\lambda^* > \lambda$, must be positive. By continuity then, there has to be a value $L^{**} \in (0, L^*)$ such that the principal eigenvalue is zero. But then (44) is satisfied for $L^{**} < L^*$, which is a contradiction to the choice of L^* . \square

References

- Alqawasmeh Y (2017) Models for persistence and spread of structured populations in patchy landscapes. PhD thesis, University of Ottawa
- Aronson DG, Weinberger HF (1975) Nonlinear diffusion in population genetics, combustion and nerve propagation. In Proceedings of the tulane program in partial differential equations and related topics. Lecture notes in mathematics, vol 466. Springer
- Berestycki H, Hamel F (2002) Front propagation in periodic excitable media. *Commun Pure Appl Math* 55(8):949–1032
- Berestycki H, Hamel F, Roques L (2005) Analysis of the periodically fragmented environment model: I-species persistence. *J Math Biol* 51:75–113
- Berestycki H, Hamel F, Roques L (2005) Analysis of the periodically fragmented environment model: II-biological invasions and pulsating travelling fronts. *J Math Pures Appl* 84:1101–1146

- Berger J (1986) Wild horses of the great basin: social competition and population size. University of Chicago Press, Chicago
- Cantrell RS, Cosner CG (2003) Spatial ecology via reaction–diffusion equations. Wiley, London
- Caswell H (2001) Matrix population models. Sinauer Associates Inc., Sunderland
- Congdon JD, Dunham AE, Van Loben Sels RC (1993) Delayed sexual maturity and demographics of blanding’s turtles (*emdoidea blandingii*): implications for conservation and management of long-lived organisms. *Conserv Biol* 7:826–833
- Congdon JD, van Loben Sels RC (1991) Growth and body size variation in blanding’s turtles (*emydoidea blandingi*): relationships to reproduction. *Can J Zool* 69:239–245
- Congdon JD, Van Loben Sels RC (1993) Relationships of reproductive traits and body size with attainment of sexual maturity and age in blanding’s turtles (*emydoidea blandingii*). *J Evol Biol* 6:317–327
- Cruywagen G, Kareiva P, Lewis MA, Murray J (1996) Competition in a spatially heterogeneous environment: modeling the risk of spread of a genetically engineered population. *Theor Popul Biol* 49:1–38
- Cushing JM (1998) An introduction to structured population dynamics. SIAM, Bangkok
- Du Y (2006) Order structure and topological methods in nonlinear partial differential equations. Vol 1: maximum principles and applications. World Scientific Publishing, Singapore
- Fang J, Lan K, Seo G, Wu J (2014) Spatial dynamics of an age-structured populations of asian clams. *SIAM J Appl Math* 74(4):959–979
- Fisher R (1937) The advance of advantageous genes. *Ann Eugen* 7:355–369
- Garlick MJ, Powell JA, Hooten MB, MacFarlane LR (2011) Homogenization of large-scale movement models in ecology. *Bull Math Biol* 73:2088–2108
- Garlick MJ, Powell JA, Hooten MB, MacFarlane LR (2014) Homogenization, sex, and differential motility predict spread of chronic wasting disease in mule deer in southern Utah. *J Math Biol* 69:369–399
- Gillanders BM, Able KW, Brown JA, Eggleston DB, Sheridan PF (2003) Evidence of connectivity between juvenile and adult habitats for mobile marine fauna: an important component of nurseries. *Mar Ecol Prog Ser* 247:281–295
- Gurtin ME, MacCamy RC (1981) Diffusion models for age-structured populations. *Math Biosci* 54:49–59
- Hastings A, Gross LJ (2012) Encyclopedia of theoretical ecology. University of California Press, California
- Hernandez GE (1988) Dynamics of populations with age-difference and diffusion: localization. *Appl Anal* 29:143–163
- Hernandez GE (1998) Age-density dependent population dispersal in \mathbb{R}^n . *Math Biosci* 149:37–56
- Kierstead H, Slobodkin LB (1953) The size of water masses containing plankton blooms. *J Mar Res* 12:141–147
- Kolmogorov AN, Petrovskii IG, Piskunov NS (1937) A study of the equation of diffusion with increase in the quantity of matter, and its application to biological problem. *Bjul Moskovskovo Gos Univ* 17:1–72
- Liang X, Zhao X-Q (2010) Spreading speeds and traveling waves for abstract monostable evolution systems. *J Funct Anal* 259:857–903
- Lui R (1989) Biological growth and spread modeled by systems of recursions. A. Mathematical theory. *Math Biosci* 93:269–295
- Lutscher F, Lewis MA (2004) Spatially-explicit matrix models. *J Math Biol* 48:293–324
- Lutscher F, Lewis MA, McCauley E (2006) Effects of heterogeneity on spread and persistence in rivers. *Bull Math Biol* 68:2129–2160
- Maciel G, Cosner CG, Cantrell RS, Lutscher F Evolutionarily stable movement strategies in reaction–diffusion models with edge behavior. *J Math Biol* (submitted)
- Maciel G, Lutscher F (2013) How individual movement response to habitat edge effects population persistence and spatial spread. *Am Nat* 182:42–52
- Maciel G, Lutscher F (2015) Allee effects and population spread in patchy landscapes. *J Biol Dyn* 9(1):109–123
- Metz JAJ, Diekmann O (1986) The dynamics of physiologically structured populations. Lecture notes in biomathematics, vol 68. Springer, Berlin
- Musgrave J, Lutscher F (2014) Integrodifference equations in patchy landscapes I: Dispersal kernels. *J Math Biol* 69:583–615
- Musgrave J, Lutscher F (2014) Integrodifference equations in patchy landscapes II: Population level consequences. *J Math Biol* 69:617–658
- Musgrave JA (2013) Integrodifference equations in patchy landscapes. PhD thesis, University of Ottawa
- Neubert MG, Caswell H (2000) Demography and dispersal: calculation and sensitivity analysis of invasion speed for structured populations. *Ecology* 81(6):1613–1628

- Othmer HG (1983) A continuum model of coupled cells. *J Math Biol* 17:351–369
- Ovaskainen O, Cornell SJ (2003) Biased movement at a boundary and conditional occupancy times for diffusion processes. *J Appl Probab* 40:557–580
- Paterson JE, Steinburg BD, Litzgus JD (2012) Revealing a cryptic life-history: differences in habitat selection and survivorship between hatchlings of two turtle species at risk (*glyptemys insculpta* and *emidoidea blandingii*). *Wildl Res* 39:408–418
- Shigesada N, Kawasaki K, Teramoto E (1986) Traveling periodic waves in heterogeneous environments. *Theor Popul Biol* 182:143–160
- Singh RS, Krimbas CB (eds) (2000) *Evolution genetics: from molecules to morphology*. Cambridge University Press, Cambridge
- Skellam JG (1951) Random dispersal in theoretical populations. *Biometrika* 38:196–218
- Stenseth NC, Lidicker WZ (eds) (1992) *Animal dispersal: small mammals as a model*. Springer, Berlin
- Thieme H (2003) *Mathematics in population biology*. Princeton University Press, Princeton
- Turchin P (1998) *Quantitative analysis of movement: measuring and modeling population redistribution in animals and plants*. Sinauer, Sunderland
- Weinberger HF, Lewis MA, Li B (2002) Analysis of linear determinacy for spread in cooperative models. *J Math Biol* 45:183–218
- White JW (2015) Marine reserve design theory for species with ontogenetic migration. *Biol Lett* 10:1054
- Yurk B, Cobbold C (2018) Homogenization techniques for population dynamics in strongly heterogeneous landscapes. *J Biol Dyn* 12(1):171–193
- Xin J (2000) Front propagation in heterogeneous media. *SIAM Rev* 42:161–230
- Zhao X-Q (2009) Spatial dynamics of some evolution systems in biology. In: Du Y, Ishii HH, Lin W-Y (eds) *Recent progress on reaction–diffusion systems and viscosity solutions*. World Scientific, Singapore

Publisher's Note Springer Nature remains neutral with regard to jurisdictional claims in published maps and institutional affiliations.